NSSDC/WDC-A-R&S 91-29

The NASA/National Space Science Data Center

Trapped Radiation Environment Model Program

(1964-1991)

James I. Vette

November 1991

National Space Science Data Center (NSSDC)
World Data Center A for Rockets and Satellites (WDC-A-R&S)
National Aeronautics and Space Administration
Goddard Space Flight Center
Greenbelt, Maryland 20771

Contents

1

INTRODUCTION

With the launch of the first artificial satellite on October 4, 1957, humankind had opened a new frontier for its activities. It was necessary to understand this new environment to learn how to survive for specific intervals of time, since future endeavors would require the placement of new equipment and, eventually, humans into that environment to successfully pursue these goals. The first satellites of both the U.S.S.R. and the United States carried instruments capable of measuring energetic charged particles, so by mid-1958 it was established that the geomagnetic field was capable of trapping particles to produce a radiation belt. Thus, the trapped radiation environment was a reality that became a factor in all space program planning.

This document will detail the major effort that NASA, initially with the help of the United States Air Force (USAF), carried out for 27 years to synthesize the experimental and theoretical results of space research related to energetic charged particles into a quantitative description of the terrestrial trapped radiation environment in the form of model environments. In this document the effort will be called the Trapped Radiation Environment Modeling Program (TREMP). In chapter 2 the historical background leading to the establishment of this program is given. Also, the purpose of this modeling program as established by the founders of the program is discussed. This is followed in chapter 3 by the philosophy and approach that has been applied in this program throughout its lifetime. As will be seen, this philosophy led to the continuation of the program long after it would have expired. The highlights of the accomplishments are presented in chapter 4. A view to future possible efforts in this arena is given in chapter 5, mainly to pass on to future workers the differences that are perceived from these many years of experience. Chapter 6 is an appendix that details the chronology of the developments of TREMP. Finally, the references, which document the work accomplished over these years, are presented in chapter 7.

2

HISTORICAL BACKGROUND AND PURPOSE OF PROGRAM

Most of the scientific instruments that had been flown in space from October 4, 1957, to July 9, 1962, were concerned with energetic protons and electrons. A general understanding of this environment was available from the results of these measurements. However, there could be large differences, at least by a factor of 10, when attempting a quantitative comparison between various measurements. This was apparent to the National Aeronautics and Space Administration (NASA) and the USAF as they received proposals from contractors in response to requests for proposals (RFPs) concerning new space projects. The engineering responses to such a variance in the radiation environment caused great difficulty in evaluating such proposals. This resulted from the fact that spacecraft shielding, power design, orbit selection, and operating lifetime were influenced by the radiation environment. Thus, the need to obtain a "best" and uniform quantitative description of the trapped radiation environment (TRE) from the available measurements was highly desirable to a number of elements of several countries' space programs.

In 1958 the U.S. began the testing of one kiloton nuclear detonations at altitudes above 200 km. Three such explosions produced short lived artificial radiation belts. Hess (1968) has provided an unclassified history of these and the additional four artificial belts produced by the U.S.S.R. and the U.S. in 1962. By far the most dramatic of the seven was the U.S. Starfish detonation on July 9, 1962. This 1.4 MT bomb, detonated at 400 km above Johnston Island in the Pacific Ocean, injected enough fission spectrum electrons (energies up to about 7 MeV) to increase the fluxes in the inner Van Allen belt by at least a factor of 100, and effects out to 5 Earth radii were observed. These electrons would dominate the inner zone for five years and would be detectable, in specific energy-space pockets, for about eight years. Shortly after Starfish ten satellites were affected by the radiation damage. For example, Ariel I went out of operation one week after Starfish, and TRAAC ceased shortly thereafter. The Orbiting Solar Observatory (OSO) 1 suffered power degradation but was able to operate at least another year. Telstar 1, which was launched on July 10, 1962, lasted less than one year because of radiation damage, although it was planned to last for several years.

Starfish had thrust the radiation problem to the forefront. There was now an extreme interest in understanding the radiation belts from a quantitative standpoint as well as from the physics. Besides the satellites mentioned above, Injun 1 and Cosmos V were in orbit prior to Starfish. Using the data from these five or six satellites, Wilmot Hess, then chief of the Theoretical Division at Goddard Space Flight Center (GSFC), began making models of the inner belt, both for electrons and protons. These models were denoted as E1, E2, etc., and P1, P2, etc., and were distributed informally by letter.

Two satellites were launched specifically to study Starfish as soon as possible following the initial results; these were Explorer 15 (October 27, 1962) by NASA and STARAD (October 26, 1962) by USAF. In addition, the regularly planned Injun 3 was launched on December 13, 1962, along with Relay 1, an experimental communications satellite equipped with a trapped radiation instrument package. Telstar 2 was launched on May 7, 1963, to replace Telstar 1, as AT&T's experimental communications satellite. Dr. Alois Schardt, then at the Advanced Research Projects Agency in the Vela Satellite Program, started the piggyback series on the Vela launches to monitor the Van Allen belts for Starfish and any new injections. These would appear as part of the Environmental Research Satellite (ERS) series, i.e., ERS 12, ERS 13, ERS 17, ERS 18, with the first being launched on October 17, 1963. In addition, there were a number of piggyback experiments being flown on USAF classified missions to make TRE measurements. Explorer 26, a follow-on to Explorer 15, and Relay 2 were other satellites whose energetic particle payloads can be considered as a direct result of Starfish. The first long-lived radiation belt monitor was launched on September 28, 1963, on board the U.S. Navy navigation satellite designated 1963-38C, which contributed data through 1968 to the National Space Science Data Center (NSSDC) archive. Thus, there was a tremendous amount of data coming from space related to the TRE by late 1963 from the impetus of Starfish. By 1970 the amount would fall to a mere trickle except for two classes of orbits, i.e., the geostationary and the polar meteorological.

During a technical meeting at GSFC in December 1963 where the latest results on Starfish were being presented, Hess arranged a private meeting with the key members of the experimental teams making TRE measurements to identify a person (or persons) acceptable to them as a body to synthesize their data for the purpose of producing TRE models for the space engineering and science communities. Since this would require access to their data long before the proprietary data period would end, this was a very sensitive matter requiring full understanding and proper handling. As a result of this process, I was contacted by Dr. George F. Pelper, then a NASA Headquarters consultant to Dr. John E. Naugle, director of physics and astronomy, Office of Space Science and Applications, to explore my interest in this task. I was then at the Aerospace Corporation in the Vela Satellite Program Office as manager for nuclear physics and had recently co-headed (with a USAF colonel) a joint USAF/Aerospace Corporation study involving trapped radiation and its effects on space systems. In addition, being at Aerospace Corporation made it convenient for the USAF to jointly fund the effort and for NASA to expedite the initiation of the program. The funding from NASA would be from Naugle's office as well as from J. Warren Keller's office within the Office of Advanced Research and Technology. The program would be run from Keller's office by Art Reetz, Jr. Based on a number of factors, including the leading role I was playing in the Vela ERS piggyback series, I accepted the job and felt honored to be chosen to discharge this responsibility for my scientific community.

3

PHILOSOPHY AND APPROACH

There were nine U.S. groups actively involved in TRE measurements at the end of 1963 (there would be a few others later). These were Aerospace Corporation, Air Force Cambridge Research Laboratory (AFCRL) (changed to the Air Force Geophysics Laboratory [AFGL] and recently to the Phillips Laboratory), Applied Physics Laboratory (APL), Bell Telephone Laboratories (BTL), GSFC, Lawrence Livermore Laboratory (LLL), Lockheed Missile and Space Corporation (LMSC), the University of California at San Diego (UCSD), and the University of Iowa (U. Iowa). Each had agreed in principle to provide data on an as-soon-as-reasonable schedule to TREMP. Since the number of groups was small, a direct working relationship with each group would be established when data from that group were solicited by the TREMP effort. During this process it was explicitly made clear to each group that the only use that would be made of the data would be for TRE modeling purposes. This cleared the air that no pre-empting of proprietary rights would occur by publishing physical interpretations of the data or by passing data on to others. Calibration data were always sought so that as one developed a TRE model (TREM) the proper conversion of the observed quantities, such as counting rate, to physical units could be done in a consistent fashion. It was agreed that the models would not have to be "approved" by the data contributors but that the treatment of the data would be given in the documentation of the model. It was decided by the TREMP to show the comparison of the model with all data used in its construction; this would be the best way to display the accuracy of the model, which is tantamount to the inaccuracy of the ensemble of data sets but not affected by a single errant data set. Additionally, it was decided that only those physical principles that were valid and dominant most of the time would be used in the models; this would prevent the models from being representative of certain analysis camps as opposed to general applicability. TREMP made no demands on the format in which the data were supplied. Instead, TREMP selected from what the Principal Investigator (PI) had available that which was best suited for the work.

Other areas of the radiation environment—namely, solar flare protons, galactic cosmic rays, trapped particles with charge greater than one, and plasma—were generally excluded from this work. The emphasis was to be on producing a TREM as soon as possible in a given energy-space-particle region based on data availability and environmental needs. In essence, the function of TREMP was to serve as a translator between scientists specializing in TRE measurements and the physical understanding of them and the space engineering and planning community. Therefore, a dialog with the users of TREMs was also established and maintained to understand their needs and the forms in which the TREMs should be presented.

With this general approach and these ground rules it was relatively easy to establish good relationships with all the PIs. Without their wholehearted cooperation it would have been very difficult to carry out the program. In the 27 years that TREMP was operative there were no serious confrontations with or animosity from any data contributor. There have been some

comparisons by others of data not used in the models with the models that have shown disagreement worthy of comment. On those occasions where such data were later submitted to TREMP, it is believed that the models and these data were brought into proper agreement or perspective. Some cases will be presented in chapter 6.

4

SUMMARY OF ACCOMPLISHMENTS

In the course of this work eight electron and eight proton models were produced. These have been designated AE-1, AE-2, AE-3, AE-4, AE-5, AE-5 Projected (AE-5P), AE-6, AE-8, AP-1, AP-2, AP-3, AP-4, AP-5, AP-6, AP-7, and AP-8. There was an interim model AEI-7HI and AEI-7LO that was generated rapidly to accommodate some important results that later were shown to be erroneous. This model never had the quality of the other models and was subsequently withdrawn from distribution. The background for this interim model is given in chapter 6. Besides these formal models there were three other efforts that resulted in two ancillary models and the verification of the latest inner zone model. The first of these was the Starfish decay (SFD) model that utilized much of the data used in the AE-5 model development as well as seven other experiments. This SFD model, besides standing on its own, was used to produce, without new data, the models AE-5P and AE-6. A second model, based on a literature review, was concerned with the plasma environment encountered in the orbit for the International Sun-Earth Explorer (ISEE) 1/2. This was the only modeling effort within TREMP that dealt with plasma data. The other effort is called the Inner Zone Study (IZS) here and was the analysis of data from eight satellites verifying the validity of the AE-5P and AE-6 models.

The total data suite used in TREMP is presented in Table 1 (see page 34 and subsequent pages). This is organized chronologically by satellite, which is given in the second column. The first column contains the PI with institutional affiliation. The third column is equivalent to the experiment flown but does not follow the usual experiment name. It is based on the type of instrument flown. The categories of instrument considered are

Geiger-Mueller Tube (GMT)
Scintillator/Photomultiplier Tube (S/PMT)
Ionization Chamber
Solid State Detector (SSD)
Beta Ray Spectrometer (BRS)
Solid State Telescope (SSD TEL)
S/PMT Spectrometer, SSD Cluster
S/PMT Cluster

In fact, if several similar instruments were flown on the same spacecraft designated by different experiment names by the project or by NSSDC, these appear as one entry in Table 1.

As an example, consider Explorer 14 with Van Allen as the PI. There were three experiments involving GMTs, which were denoted as 302 GMT, 213A GMT, and 213B GMT; all appear in Table 1 under one GMTs entry. The type of measurement, given in the fourth column, has been categorized relative to the energy spectral characteristics and to the angular characteristics.

The spectral characteristics are denoted by threshold detector (THD), range (RAN) of energies as in typical SSD or S/PMT proton detectors, a detector sensitive to bremsstrahlung electrons as opposed to directly penetrating electrons (BREM), differential in energy by result of magnetic focusing (DIF), and differential in energy by result of pulse height analysis (PHS). In regards to the angular characteristics, the following categories were used:

- Omnidirectional (OMNI).
- Directional (Pitch angle relative to the magnetic field vector is known for each measurement.) (DIR).
- Directional but only perpendicular to the magnetic field vector (PERP).

In the fifth column is the period of coverage for the data used in the models. In many cases this is the complete data coverage for the instrument, but not always. To obtain the complete coverage available in the NSSDC archive, for example, consult the NSSDC data catalogs (86-01 and 88-01). The sixth column deals with the L (McIlwain parameter) coverage for the data used in the models. The full range of coverage of the data is usually larger than that given in Table 1. Again, the interested reader should consult the NSSDC catalogs. In the seventh column the energy range for each channel is given, followed by the letter p for protons or the letter e for electrons. These values are the ones used in the construction of the models and may not be the same as those published by the PI and his associates. They are based on calibration data, when available, and the model spectrum; thus, they are the most consistent parameters to use in conjunction with a given model. In those instances where two values are shown, there were different values used in different models. The instrument may also have a proton channel (not shown, since it was not used in a model) if e is given or vice versa. Finally, the last column indicates the models or studies in which the data were utilized. The entries AE-5P and AE-6 do not appear. These models employed AE-5 and the SFD entries.

A summary of Table 1 is in order at this time and is given in Table 2 (see page 41). There are 43 satellites. There are 55 PIs listed where the same named PI is counted once for each spacecraft. Thus, Van Allen is counted four times for Explorer 4, Explorer 12, Explorer 14, and Injun 5. There are 265 energy channels of information used, and the average number of months of data for each channel is 6.2. Naturally, this number was lower for the early days and generally increased with time. The first satellite used was launched on July 26, 1958 (Explorer 4), and the last (ATS 6) on May 30, 1974, with the data extending to June 1978. Thus, data extending over a period of 20 years were ingested to obtain the quantitative models constructed by TREMP.

A brief summary of the 16 TREMs is given below; more specifics will be presented in chapter 6. Although the data obtained to construct the models came in the many forms given in Table 1, the final results were presented in the THD, OMNI form.

AE-1 covered inner zone electrons (L region 1.2-3.0) with energies from 0.3 to 7.0 MeV with an epoch date of July 1963. Starfish decay was the only known time dependence. The energy spectrum was independent of the magnetic field intensity, B. The protons were first broken into the four energy regions: 4-15, 15-30, 30-50, and above 50 MeV because the spectrum was B dependent. All proton spectra within each region were represented by an exponential whose e-folding parameter, E_O, was a function of B and L. The naming of these four models was in the order in which they were constructed. Thus, the correspondence to the monotonic sequence above is AP-4, AP-2, AP-1, AP-3. Since trapped protons are confined by the atmosphere at a sharp and relatively energy-independent inner edge and by an energy-dependent outer boundary, the L range for each proton model was different. The inner edge was about L = 1.17 and the outer L boundary was about 4.6, 3.5, 3.15, and 2.9, in monotonic energy order. The known time dependences at that time were caused by solar cycle effects and nonadiabatic redistribution near the outer boundary resulting from large magnetic disturbances. An epoch of September 22, 1963, was chosen because on the following day a large redistribution occurred. This set of four models was formally documented by Vette (1966a) and sent to users in early

1965. Presentations of this work were given in late 1964 and in 1965 with subsequent publication by Vette (1965a, 1965b, and 1966b).

AE-2, the next model constructed, provided a new epoch of August 1964 for the inner zone and made the first attempt at modeling the outer zone electrons. The time average of the logarithm of the outer zone electron flux was used as the model variable to handle the large time variations. The L range was 1.1-6.3 and the energy range was 0.04-7.0 MeV. This was formally documented by Vette et al. (1966).

AE-3 was constructed from elliptical satellite data to provide an electron environment in the geostationary orbit prior to any direct measurements in this region. This extended the treatment on time variations, developed the log-normal distribution approach, and predicted that no solar cycle flux effects within a factor of 2 (the estimated error in the data based on intercomparison) were present in this region. The standard deviation of the logarithm of the flux, σ, which was the only additional parameter needed for the statistical description, depended on L and energy. This work was presented at the fall 1966 American Geophysical Union (AGU) meeting in Los Angeles as an invited paper, and formal documentation was given by Vette and Lucero (1967).

The work for AP-5 was under way by J. H. King at this time. At the end of 1966 J. I. Vette left to become the director of NSSDC, and with the exception of the AP-5 work, TREMP was moved to NSSDC. NASA agreed that TREMP fit into the general concept for NSSDC by providing useful professional activity for the scientific staff, encouraging data acquisition at an early stage, and providing a useful data product for the NSSDC user community. NASA continued to support TREMP separately two more years, but then it was carried on within the NSSDC budget until its termination by NSSDC management in 1991. AP-5, which covered the energy range from 0.1 to 4.0 MeV, was completed at Aerospace Corporation in 1967 by King (1967). This model extended the L range to the geostationary orbit region ($L \approx 6.6$) and used an exponential energy spectrum similar to the earlier proton models.

Although work was begun in 1967 on AE-4 as a comprehensive outer zone model employing and extending the techniques employed in AE-3, this massive task was not completed until 1972. New proton data allowed an update of some of the earlier models. By employing a power law spectral function instead of an exponential one, Lavine and Vette (1969) were able to combine the 4-30 MeV range into a new model, AP-6. This was based on data covering parts of the time period December 1962-February 1965 with avoidance of times following redistributions. A wealth of new data in the region above 50 MeV allowed AP-3 to be updated to AP-7. Although the data studied covered parts of the time period August 1961-July 1966, an extensive study of time variations allowed an epoch of January 1969 to be set for this model. Solar cycle effects at very low altitude could not yet be incorporated, however. This model was documented by Lavine and Vette (1970).

The formal documentation of the models was done through the NASA Special Publication Series. When NASA Headquarters direct support ceased, it was decided to carry on the publication of the models through NSSDC, since the time to publish would be much reduced. Also, documentation of work in progress was feasible. Thus, Teague (1970), Singley (1971), and Teague and Vette (1971) published work connected with the coming electron environments, AE-4 and AE-5.

By August 1972, AE-4 was completed. This covered the L region 3-11 and the energy range from 0.04-4.85 MeV. The model contained a local time variation as a function of L, energy, and local time. The spectral function was tabular and independent of B. The statistical parameter σ depended on L and energy. A solar cycle effect covering the L region out to 5.5 was included, and the conclusion from AE-3 work that this effect was not present in the geostationary region was confirmed. The low altitude cutoff could not be determined from the available data, so a conservative cutoff based on a 200-km atmospheric maximum drift height was used. This model was documented by Singley and Vette (1972a, 1972b).

The inner zone AE-5 model was being developed by Teague and Vette concurrently with AE-4. This utilized data from December 1964-December 1967 and was given an epoch of October 1967 to represent a near solar maximum (SOLMAX) condition. The L region covered was 1.2-2.8 and the energy range was 0.04-4.0 MeV. Three time effects were studied and used to bring flux levels to the epoch time; these were magnetic substorms, SFD, and solar cycle. A BLOCK DATA statement was used to represent the combined AE-4 and AE-5 numerically, as opposed to the tabular presentation on computer cards used for the previous models. This compression was necessary to reduce storage requirements. The model was documented by Teague and Vette (1972), and further instruction on the use of the model with associated programs developed by TREMP was given by Teague et al. (1972).

The Starfish decay model developed by Teague and Stassinopoulos (1972) in this period was the main tool for the next electron work. A solar minimum (SOLMIN) inner zone model was needed to accompany AE-4MIN. Since the next SOLMIN was 1975, one had to remove the Starfish residue from the AE-5 fluxes. It was known that all Starfish electrons would disappear before 1975. In addition, the solar cycle variation had to be utilized to adjust the natural levels from SOLMAX to SOLMIN. This model was AE-5P (Teague and Vette, 1974). Comparisons of the earlier AE-2 and AE-3 models with the AE-4 and AE-5 models were provided by Hilberg and Vette (1974). The period from 1972-1974 was the apex of TREMP in terms of personnel, resources, and productivity.

The next SOLMAX of 1980 required the removal of the Starfish residue from AE-5 without further alteration. This resulted in AE-6 (Teague et al.,1976). Although this was an easier task than AP-5P, it appeared later since it was not required by the user community as soon.

AP-8 was a long-term effort to bring all the proton models under one common approach and include the new data available since 1970. Since storage capacity had become larger with the advance of computer technology, a decision was made to use a completely numerical description rather than to employ analytical spectral functions. In addition, some later low altitude data permitted the first solar cycle variation to be incorporated into the proton model. This work (Sawyer and Vette, 1976) involved the large number of instruments summarized in Table 2 (see page 41) and detailed in Table 1 (see page 34 and subsequent pages).

Following the issuance of AE-4, new data became available that allowed the high energy portion of the spectrum to be corrected and to obtain a good inner edge cutoff consistent with that obtained for the inner zone. As with AP-8, this new model combined all the electron energy-space regime into one model, AE-8. A study of new inner zone data (Teague et al., 1979) showed that no changes were required in AE-5P and AE-6. Because the TREMP effort had been reduced considerably after 1977, AE-8 was not completed until 1983. The formal documentation was just recently completed (Vette, 1991).

Besides the documents that have formally described the TREMs, there have been 22 publications in books, professional journals, and documents of other agencies contributing to the literature in various aspects of TRE. These are by Vette (1965a, 1965b, 1966b, 1967, 1970a, 1970b, 1970c, 1971a, 1971b, 1972, 1979, 1989, 1990a, and 1990b), Vette et al. (1978 and 1979), Lavine and Vette (1970), Chan et al. (1977a and 1979), Sawyer et al. (1978), Lemaire et al. (1990), and Kaye (1981).

Finally, the TREMs have been supplied to users in all spacecraft launching countries and many others involved in space work. The distribution list for the TREM documentation has contained about 200 names throughout the lifetime of the program.

5

A VIEW OF THE FUTURE

The present knowledge of the TRE has been derived mainly from the data obtained during the first 12 years of the space era along with the theoretical, analytical, and modeling efforts associated with them. It has been pointed out that the first area of discovery and scientific effort in space involved energetic particles. The instruments were readily available out of nuclear physics, high-energy physics, and balloon/rocket-borne cosmic-ray work. It took nearly a decade to develop instruments for other areas such as plasma, astronomy, and Earth resources, where the main thrust has been for the past two decades. Meteorology was the only equivalent thrust to energetic particles initially, and this has continued to develop because of the economic impact of weather prediction throughout the world.

Consequently, the future for TRE research is not very bright. The effort peaked in the late 1960s, and it is unlikely that even 15% of that peak will ever occur again. The scientific interest moved to the plasma regime in the 1970s and likely will remain there. Therefore, it is imperative to understand what the state of knowledge in the TRE area is following the work of the 1960s, look at the data potentially available for near-term modeling work, and then identify what can be done to improve updating the TRE with minimum cost and impact on other space missions. It is also imperative to understand the future need for the TRE knowledge. This need is perceived to be in radiation damage to solar cells, solid state devices, and humans, for deep dielectric charging, and for backgrounds likely to be produced in sensors for missions in other disciplines.

The present knowledge of trapped protons and energetic electrons, trapped or otherwise, is reviewed first. From the radiation damage standpoint only protons with energies 5 MeV and greater and electrons 0.5 MeV and greater are important. For backgrounds to sensors, electrons down to 20 keV may be important. In the interest of brevity, references to the primary literature will not generally be given in this chapter. Primary references and other details are given in the documentation of the models cited earlier.

Knowledge of Trapped Protons

The inner boundary for protons is determined by the atmosphere, and no protons are seen much below 150 km in altitude. This lower boundary changes with the solar cycle, since the atmosphere is heated by the Sun's ultraviolet output, which increases during its more active phase. Of course, this boundary is slightly energy dependent. Since the flux gradient is very steep near this boundary and the Earth's magnetic field center of symmetry does not coincide with that of the Earth (they are different by 500 km), the precise inner boundary is complicated relative to a spherical Earth with a centered field. Thus, the lowest altitude that a proton reach-

es during its trapped trajectory is in the South Atlantic Anomaly (SAA) near the coast of Brazil. The approximate inner boundary is at a radial distance of 1.024 Earth radii (R_e).

Protons of at least 500 MeV are trapped in the magnetosphere. Once protons are too energetic, their gyroradii become too large for trapping to occur; this places the upper energy limit. The most energetic protons peak around 1.4 R_e. By the time the energy drops to 40 MeV, the peak has moved outward to 1.5 R_e. This trend continues so that 5 MeV protons peak at 1.8 R_e. The outer boundary also has the same trend with energy. 400 MeV protons reach the minimum TREM flux of 1 proton/cm^2-s at 2.1 R_e, 50 MeV at 2.9 R_e, and 5 MeV at 4.7 R_e. Thus, there is only one zone of protons. Lower energy protons extend farther out, and eventually the plasma sheet protons with an average energy of 8 keV are encountered. These lower energies are of no interest here. Protons in the range 5-15 MeV are the most important for solar cell arrays, and it requires about 30-40 MeV protons to penetrate the shielding of spacecraft and space suits. For this energy range at any given L shell, the energy spectrum hardens as one goes away from the equator. Above 50 MeV the behavior is somewhat different. The more energetic protons have a flatter equatorial pitch angle distribution than lower energy ones. The peak fluxes present a significant radiation hazard. For example, 30, 15, and 5 MeV protons have peak fluxes of 4×10^4, 1.1×10^4, 3×10^6 protons/cm^2-s.

The sources for the protons are cosmic-ray albedo neutron decay (CRAND) protons for protons energies down to about 10 MeV and from the solar wind for the lower energies. It is difficult to trace in quantitative detail the injection of solar wind protons (~ 1 keV energy) through the geomagnetic tail with inward radial diffusion producing acceleration to the observed energies. There is some difficulty getting enough acceleration to achieve the right energies. The energy spectrum of the lower energy trapped protons as a function of spatial position (L value) is consistent with radial diffusion. However, it has not been possible to compute expected fluxes with any degree of certainty. The CRAND source has been studied extensively, and detailed calculations have been made. In the early 1960s the source was found to be too weak by a factor of 20-50. However, by 1974 new neutron measurements and further theoretical refinements brought theory and observations within a factor of about ± 5 for energies above 30 MeV.

There are several known time variations for the trapped protons. The best understood is the loss into the atmosphere by the energy-loss-by-collision process at the inner boundary. A solar cycle effect, caused by the change of the density as a function of altitude over the solar cycle, has been discussed earlier (see page 13). This effect has been accounted for in the AP-8 model. However, the secular change of the geomagnetic field, which has an exponential folding time of about 1000-2000 years, begins to show up in the use of AP-8. It was pointed out by Konradi et al. (1987) that the application of the secular field with AP-8 to extrapolate up to 30-40 years in the future resulted at low altitude in fluxes that were increasing at an alarming rate and were inconsistent with observations obtained by dosimeters flown on Shuttle flights. Vette and Sawyer (1986) suggested changes in the computer program used to deliver fluxes from AP-8 that should alleviate the problem. Daly (1989) showed that this scheme reduced the change but the effect was still troublesome. Later, Pfitzer (1990) showed that by using the average density encountered by protons at Space Station altitudes in the SAA as a parameter in place of the magnetic field strength, there was a proper ordering of AP-8MAX and AP-8MIN fluxes. It was known from the work of the 1960s that the proton flux at low altitudes was proportional to the inverse of the average density. Pfitzer's work uses only the bounce and drift motion of the protons; it is recognized that the gyro motion must also be used at still lower altitudes. Since this additional motion increases significantly the computational time, it should be included discretely.

A point to be made here is that existing knowledge can be combined to treat new effects satisfactorily in some cases. However, there remain significant problems relating theory to observations. The combination of proton sources, diffusion, acceleration, and other possible loss mechanisms cannot be used to accurately predict the future situation in most of the region where energetic protons reside. In addition, there are known redistributions of protons at the

energy-dependent outer edge caused by large magnetic storms. The intermittent coverage of the 1960s did not permit the detailed study of the time behavior of these events, but it appears the perturbations in the flux returned to zero after months of time. The periods were long enough that it was clear that non-adiabatic effects had occurred. Smaller adiabatic effects have also been seen that follow magnetic perturbations in a known manner. The energetic protons in the 5-500 MeV show a great deal of long-term stability over a decade or so, but any long-term effects other than those produced by the secular changes in the geomagnetic field and the solar cycle changes in the atmosphere are completely unknown.

Knowledge of Energetic Electrons

Since the most energetic electrons are the most effective in producing deep dielectric discharges, this chapter includes a discussion of Jovian electrons, which are not trapped in the magnetosphere but are present there at certain times.

Energetic electrons are found nearly everywhere within the magnetosphere depending on the lower energy limit chosen. The general limit for the trapped radiation models has been about 40 keV, since this is a good boundary to distinguish plasma instruments from the "energetic" particle detectors. Some solar flare proton events also contain MeV electrons that act much like these protons in gaining access to the magnetosphere. Since the solar protons dominate the radiation hazard during flare events, these solar flare electrons are of no concern here.

Since the Earth's atmosphere is the cause of the inner radial boundary, this boundary is similar to that of the protons. However, the physical mechanisms by which protons and electrons are lost are different. The main observational differences are that the electrons have a longitude dependence at low altitude while the protons do not and the lifetime of electrons is considerably shorter. Electrons are scattered by the atmospheric atoms through pitch angle scattering, a process that breaks the first adiabatic invariant. Because of this mechanism, electrons mirroring at low altitude are removed from the trapping region in the SAA, but others are scattered down to replace them; thus, a longitudinal variation is produced.

The injection of Starfish electrons provided an excellent experiment to understand the loss mechanism for electrons. At altitudes up to about L = 1.25, the atmosphere accounted for the observed decay. It is the density at the geomagnetic equator that determines this decay rate. Above this L value other processes, such as diffusion and very low frequency (VLF) emissions, become more dominant mechanisms, but quantitative agreements were not possible to obtain since neither diffusion coefficients nor power spectral densities could be determined accurately. In the inner zone from L = 1.25-2.2, the maximum lifetimes for Starfish electrons occurred at 1.6 MeV and L = 1.3 with an exponential decay time of 375 days. At L = 2 this had dropped to 100 days, and by L = 2.1 it was 50 days. By 1970 all Starfish electrons had decayed, so the AE-8 model now gives only natural electron fluxes. There are occasionally substorm injections seen diffusing in to about L = 1.8. Below this value no time variations other than the solar cycle flux effect are expected. This inner zone region is summarized and characterized by the following peak integral omnidirectional fluxes.

Threshold Energy (MeV)	Peak Flux (e/cm^2-s) SOLMAX	SOLMIN	L Value of Peak SOLMAX	SOLMIN
0.04	8.33E8	5.71E7	4.70	5.59
0.50	1.12E7	9.44E6	4.61	5.06
1.00	3.85E6	2.96E6	4.39	4.74
3.00	1.27E5	7.50E4	3.72	4.20
7.00	5.01E0	5.01E0	3.18	3.18

The solar cycle effect is seen in the fluxes below 0.7 MeV with the position of the peak flux moving inward at SOLMIN; no such changes occur for the higher energy electrons in this region.

The L region between 2-3 is usually referred to as the slot. For the time averaged fluxes it contains the trough of the equatorial fluxes for the energy range 0.4-4.5 MeV, as will be illustrated later. Below these energies the minimum occurs further outward. The lifetimes of electrons in the slot have been measured to be from 15 to 50 days with lower values as L increases. Because only a few injection events from the tail reach this region, it is a difficult one to model in terms of average values; nine-month averages have been shown to vary by as much as a factor of 10. However, the injection events reaching this region can produce flux increases by factors of 30-100. It has been shown that the injection events reaching the region produce total energetic electron content values proportional to the magnetic D_{st} index. It has also been shown that many events do not penetrate this deeply into the magnetosphere, independent of the D_{st} value. Thus, D_{st} cannot be used to estimate the flux reliably. A summary of the trough situation for the long-term time averaged integral omnidirectional fluxes is as follows.

Threshold Energy (MeV)	Trough Flux (e/cm^2-s) SOLMAX	SOLMIN	L Value of Trough SOLMAX	SOLMIN
0.04	4.14E7	1.42E7	3.05	3.40
0.50	2.50E6	6.47E5	2.80	2.75
1.00	3.88E4	3.79E4	2.24	2.26
3.00	4.06E0	4.06E0	2.32	2.32

It should be noted that the 0.04 MeV trough is located outward from the slot. The solar cycle effect reaches up to 1.00 MeV at L = 2.25, and before leaving the slot all energies exhibit this effect. Fortunately, the flux levels are generally low enough in the slot that radiation damage is not a factor. If one considers the electron lifetimes in this region, which are believed to be the result of the presence of VLF whistlers, and the diffusion velocity, which varies as L^{-8}, then most electrons diffusing across the slot should be lost in this region. From the solar cycle effect seen in the electrons below 0.7 MeV in the inner zone, it is suggestive that these electrons are able to diffuse through to the inner zone, while the higher energy ones do not.

As one moves outward from the slot into the outer electron zone, one finds another peak in the electron fluxes. This is summarized below for the time averaged integral omnidirectional flux.

Threshold Energy (MeV)	Peak Flux (e/cm^2-s) SOLMAX	SOLMIN	L Value of Peak SOLMAX	SOLMIN
0.04	8.33E8	5.71E7	4.70	5.59
0.50	1.12E7	9.44E6	4.61	5.06
1.00	3.85E6	2.96E6	4.39	4.74
3.00	1.27E5	7.50E4	3.72	4.20
7.00	5.01E0	5.01E0	3.18	3.18

All energies show the solar cycle effect except the very highest ones for which there have been very few data. This effect disappears in the L = 5.0-6.0 range, depending on energy. The hardest electron spectrum occurs in association with the 7 MeV peak at L = 3.18. The general solar cycle effect is such that the SOLMIN peak flux is invariant, but the inner side of the peak grows during the rise to SOLMAX and pushes the observed peak inward and to higher values by as

much as a factor of 10. This is a fine detail that is difficult to see with all the time variations present but that becomes clear in the average fluxes.

The time variations in the 3.5-5 L region show large injection events with the flux rising abruptly by as much as a factor of 1000. Then there is a period of exponential decay until this is interrupted by another injection rise or by a rapid fall. The decay times at L = 4 and 5 are nearly the same, but at L = 5 one sees about three times as many injections. Decay times in this region are observed to be 15-30 days for energies above 1.5 MeV but are about 5-6 days for 0.5 MeV. The same morphology continues as one moves to higher L values, but the decay times become less and the rapid falls are more prevalent. When one looks at the geostationary region, the exponential decay segments essentially vanish, and the time structure can be characterized by many injection events of varying size (rarely exceeding a factor of 100) appearing as jagged top rectangular waves. As one moves on to greater distances, the pattern looks more chaotic, and there are periods where there is no discernible flux.

Qualitatively, the substorm injection process is well understood. During certain periods, particularly when the interplanetary magnetic field has a negative Z component in a geocentric solar magnetic coordinate system, magnetic energy is stored in the geomagnetic tail. This can be monitored nicely in the geostationary orbit and is detected by the character of the magnetic field seen there as switching from a dipole-like to a tail field. Some triggering mechanism, which is not clear at the present but is conjectured as resulting from plasma instabilities, causes the magnetic field to revert back to its dipolar configuration. In this process some of the stored energy is transferred rapidly to the particles. After this, diffusion occurs because of all the magnetic and electric turbulence so that the inward diffusing particles gain additional energy. Thus, if one considers some plasma sheet electrons winding up at L = 8.5 with 0.05 MeV of energy, then after diffusion to L = 3.2, the most energetic region, they would have an energy of about 3 MeV. It is known from the geostationary observations that some 500-1000 such injections occur per year. There are loss mechanisms resulting from wave particle interactions and other processes that produce pitch angle scattering. These produce the rapid loss and pseudo-exponential decays seen during the injection events in the L = 3.5-5 region.

It is impossible to predict the flux levels in the outer zone because of the complex process outlined here. However, the long-term time average (about nine months) reveals the behavior described above, and at geostationary the fluxes do not exhibit solar cycle effects. There AE-8 gives values of 4.60E7, 2.90E6, 4.80E5, and 3.70E3 electrons/cm^2-s for 0.04, 0.50, 1.00, and 3.00 MeV. Starting around 4 MeV, the fluxes are no longer constant in the long-term average but may vary as much as a factor of 5. This variation is stochastic in nature and bears no correlation with the solar cycle. It does have some correlation with the presence of high speed solar wind streams. From the modeling standpoint, this region has an error similar to that encountered in the slot region.

The local time variation seen in the fluxes in the L range > 3 (and most clearly at geostationary orbit) is produced by the current systems in the magnetosphere external to the Earth's surface. In terms of the TREMs, these variations result from a coordinate system chosen for the user's efficiency.

At the geostationary region there have been observations of bursts of very energetic electrons up to 10-15 MeV. It has been suggested that these could be of Jovian origin or possibly internal magnetospheric accleration resulting from high speed solar wind streams. Cosmic-ray instruments in the near-Earth interplanetary medium have measured Jovian electrons directly. These are seen mainly every 13 months when Jupiter and the Earth are in the same interplanetary magnetic flux tube. The average omnidirectional integral Jovian electron flux is given approximately by

$$J_{je}\ (>T) = 1140\ T^{-2}\ ;\ T \text{ in MeV}$$

so that one finds fluxes of 42, 10, and 2.5 electrons/cm^2-s for > 5, > 10, and > 20 MeV. Bursts of such electrons might be the cause of some deep dielectric charging anomalies. On the basis of studies of solar proton access to the magnetosphere, one could expect that the transport of these particles into the magnetosphere may occur without delay or loss. Unfortunately, simultaneous observations at geostationary and in the nearby interplanetary medium have not been made, as they have for protons. It is possible that the dominant source of electrons seen in the magnetosphere greater than 5 MeV is Jupiter; however, these electrons do not become permanently trapped, based on many years of solar proton observations within the magnetosphere.

Beyond geostationary the stable trapping region extends to the magnetopause boundary on the day side (average distance = 11 R_e), and at local midnight this boundary is nearer to 7 R_e where the pseudo-trapping region begins. Thus, at most local times the stable trapping region is inside 7.5 R_e, except very near the nose of the magnetopause. The local time averaged 0.25 MeV electrons of AE-8 end at an average distance of 11.5 R_e, which means both trapped and pseudo-trapped particles are counted. The 0.5 MeV flux drops to the model lower limit at 10.5 R_e. The pseudo-trapping region is defined by the inability of the particles to execute complete drift motion around the Earth. Particles starting in the midnight sector will drift out through the magnetopause boundary as the particle moves to the dayside magnetosphere. This pseudo-trapping region extends to about 12.5 R_e in the midnight sector; its outer boundary coincides with the inner boundary of the plasma sheet. The presence of electrons in energy bands around 350 keV and even up to 1.5 MeV have been seen, but average fluxes are very low. These outlying regions have large fluctuations that are difficult to model because of the lack of data. However, except for background problems for certain missions, the fluxes are low enough that radiation damage is not a problem.

Prospective Data for Near-Term Modeling

During the past 10-15 years the drop-off of scientific satellites for TRE measurements has been partially compensated for by operational or one-shot applications satellites. This discussion will be restricted to the payloads launched in 1976 or later and to the more recent payload versions for operational missions. Only the measurements likely to be available for TRE modeling will be identified. These will be organized by satellite orbit into four regions:

- Low altitude polar meteorological.
- Synchronous (but not geostationary).
- Geostationary.
- Highly elliptical.

The National Oceanographic and Atmospheric Administration (NOAA) Television and Infrared Observation Satellite-N (TIROS-N) series was first launched in 1978 with a total of nine satellites in the series with two left to be launched. These are in near circular orbits around 850 km at about 99° inclination. The Space Environment Monitor (SEM) has three directional electron channels at greater than 0.03, 0.01, and 0.3 MeV as well as 14 proton channels. These proton channels are of more interest. The Medium Energy Proton and Electron Detectors (MEPEDs) are three separate omnidirectional devices covering the range 16-215 MeV. The High Energy Proton and Alpha Detector (HEPAD) is a counter telescope with a 24 half angle covering the 370-850 MeV interval with three channels and a greater than 850 MeV channel. This last channel is of no use to TRE. Near equatorial coverage is only made at very low L values, but all shells of interest are sampled. The data are readily available from NOAA. A long time series from overlapping instruments that can be intercalibrated should be possible. The Defense Meteorological Satellite Program (DMSP)/F7 launched in November 1983 carried a Space Radiation Dosimeter that obtained good measurements of electrons and protons until July 1988. These measurements were of integral omnidirectional fluxes. The two useful electron channels were greater than 1 and 2.5 MeV. For protons the channels were

greater than 20, 35, 51, and 75 MeV. This long data base showed an increase of 6%-7% for the inner zone proton channels but constant for the electron ones. Thus, the proton data should provide some quantitative information about the solar cycle effects. The satellite was in the same type of orbit as the NOAA series, so the radiation belt coverage was the same. The four-second data are available at NSSDC.

The International Ultraviolet Explorer (IUE) astronomy satellite carried a Particle Flux Monitor for operational purposes. This was a solid state detector with a 16° half angle field of view that measured electrons greater than 1 MeV. Pitch angle information can be obtained from the known altitude of the spacecraft. The orbit of the satellite is 29° inclination with a 45,000-km apogee and a 26,600-km perigee. Data are available from NSSDC from November 1980 to the present time. The effective radiation belt coverage is from L = 5.4-10 mainly in the magnetic mid-latitude range. The long data base provides a unique monitor of outer zone electrons off the equator. The Spacecraft Charging at High Altitudes (SCATHA) (STP P78-2) satellite was in a similar orbit to IUE and carried a full complement of energetic electron detectors. Data books have been made for the period March 1979-May 1980, but it is doubtful that digital data for this satellite will ever be available for modeling. Consequently, no further discussion is given here.

Starting in 1976, the USAF began a series of operational satellites that carried a Charged Particle Analyzer (CPA) covering the trapped electron and proton ranges in the geostationary region. The low energy electron range 0.03-0.3 MeV was covered by six energy channels in a fan-shaped way that provided omnidirectional coverage. The 0.2-2 MeV electron range was covered in six channels, and here the measurements are directional. Trapped protons from about 0.07-2 MeV are covered by 14 energy channels; these are directional measurements. Solar proton channels are not addressed here. In June 1979 an additional electron instrument was added, the Spectrometer for Energetic Electrons (SEE). This covers the energy range 3-15 MeV in four channels. The measurements are directional. These two sets of instruments have provided a continuous set of observations that are available in the geostationary region. The SEE data are not yet readily available, since energy calibrations are still being analyzed. The CPA data are available through the Los Alamos National Laboratory (LANL), and NSSDC has a copy through 1985. There is one channel of electron data greater than 2 MeV directional to the satellite spin vector on the Geostationary Operational Environmental Satellite (GOES)/Geostationary Meteorological Satellite (GMS) weather satellites starting in September 1980. As an independent check on the LANL data, this may be useful, but the LANL data provide a much more comprehensive set for the serious modeler.

There are very few data available in the more distant regions of the magnetosphere. The International Sun-Earth Explorer (ISEE) 1 and 2 Medium Energy Particle Instrument (MEPI) is worthy of mention here. This instrument provided measurements of electrons and protons in the 0.02-1.2 MeV range and protons up to 2 MeV. The ISEE 1 data covered the period from November 1977-September 1979 and provided much better coverage for electrons above 0.3 MeV. These data have been analyzed for TRE modeling by Tranquille and Daly (1988), who are also analyzing the ISEE 2 data set covering the period November 1977-October 1987. These satellites were in the same orbit simultaneously covering the range from 22.6 down to 1.044 R_e with an inclination of about 29°. Thus, for all local times the magnetosphere was well-covered by this mother-daughter pair.

The combination of the DMSP/F7, IUE, and LANL data in the same time period provide some unique opportunities to study electrons in the L shell splitting (synchronous) region. In addition, all the data sets discussed above provide the basis for the long-term behavior of the TRE in a solar cycle era later than that of the AP-8/AE-8 analysis. The 5-15 MeV proton window so important for solar cells is not covered at all in this new era.

The Long-Term View

Because the TREMs have been in constant use since their inception in 1962 following Starfish, it is assumed here that such products of knowledge will continue to be needed. The thoughts below are given to help those charting the TREM paths for the future.

In June 1990 the Combined Release and Radiation Effects Satellite (CRRES) was successfully launched into a 16° inclination orbit with a perigee height of about 400 km and an apogee at about 6.6 R_e. From a TRE standpoint the payload is the best that has ever been flown. Besides covering the plasma and low-to-medium energy ions, the TRE electrons and protons are completely covered. Thus, protons from 0.1 to 600 MeV and electrons from 0.02 to 10 MeV are covered when the various instrument channels are combined. By virtue of the fact that the orbit is near equatorial and the instruments measure directional flux, all particles trapped on the flux tubes from the inner boundary out to the geostationary region are sampled twice every 11 hours. Thus, that whole region of the magnetosphere will be extensively monitored over the lifetime of the satellite. Assuming NASA and USAF keep this system going for its complete life, a new set of models could be produced.

The main questions then are

- How long will the spacecraft last?
- Will funding be provided to the PIs and the project long enough to build a data base suitable for modeling purposes?
- Who is going to do the modeling?

The spacecraft could last for five to ten years, but with the funding situation as it is, it will be lucky if three years of operation are achieved. Nor has the funding for data analysis on projects like this ever been adequate. SCATHA was a similar NASA/USAF project for environmental purposes (spacecraft charging). Although the spacecraft appears to have operated for over six years, very little data have reached the state where modeling can be done. An atlas containing about 14 months of plots exists, but digital data are not readily available, as mentioned earlier. It remains to be seen what will come out of this CRRES mission. It is also not clear what modeling is to be done with this data. It has already been stated that NSSDC, which has provided this service from 1967-1983 with consultation service until 1991, is now closing down its activity in this area, except for distribution of models and computer access to them. It is known from experience that this has never been, nor likely ever will be, a PI activity; the focus is different. The potential move of the Phillips Laboratory from Hanscom Air Force Base, Massachusetts, to Albuquerque, New Mexico, may be disruptive to the data processing, analysis, and modeling phases of the CRRES project.

It appears to this author that the interested groups in TRE within the space agencies need to organize themselves in an informal way to produce such model environments. This approach has worked in the astronomy area in the production of star catalogs. France, through its Stellar Data Center, the U.S. through NSSDC and GSFC, and the U.S.S.R. and Japan through suitable observatories have built a viable cooperative program. The organizations that might contribute to a TRE model construction program are

- NASA, NOAA, USAF (U.S.).
- European Space Agency (ESA)/European Space Technology Center (ESTEC).
- Institute of Space and Aeronautical Science (ISAS), National Aeronautics and Space Development Agency (NASDA) (Japan).
- Institute of Cosmic Investigation (IKI) (U.S.S.R.).

The Peoples Republic of China is not listed since the relationships in this area are not yet well-established. It should be noted that the modeler will probably have more difficulty in producing models than TREMP. The reason is that now data are not analyzed as extensively nor processed in a manner beneficial for modeling. This statement is not true for all the data

cited above but certainly applies to the average situation. Furthermore, with the field much less active now new ideas and theoretical approaches will be less prevalent.

E. J. Daly of the Mathematics and Software Division at ESA/ESTEC has been working toward a cooperative effort and funded a 15-month study in 1989-1990 to assess the TRE situation as the ground work for revitalizing the field. Some recommendations are made in the last technical note of this effort (Vette et al., 1990) and in the Final Report (Lemaire et al., 1990). It is felt that the type of TRE data from NOAA and NASDA weather satellites will continue to be available well into the future. The same is believed to be true for the USAF LANL satellites. Clearly, a fully supported Radiation Effects Satellite (CRRES minus the chemical release experiments) once every decade would define the main part of the TRE. Another recommendation is to develop some standardized, minimally intrusive instruments for piggyback rides on different mission opportunities. Some discussion of these is given in Vette et al. (1990). Many of the instruments that contributed to the TRE data base of the 1960s were of a piggyback nature. They were far from standardized, however.

6

APPENDIX: CHRONOLOGY AND REMARKS ON TREMP DEVELOPMENT

A brief summary of each of the models developed in this program was presented in chapter 4. The purpose of this appendix is to provide more detail and show how the tools and ideas grew with each of the models. Some of the facts in chapter 4 are repeated here, information from Table 2 (see page 41) is cited, and the satellites are given so that the reader can consult Table 1 (see page 34) for additional information.

The AE-1 Model

The first model produced in this program was AE-1. The eight satellites 1962 AU1, 1962 BE1, STARAD, 1962 BO1, Explorer 15, Relay 1, Injun 3, and 1963-45A carried a total of nine instrument sets that provided 45 channels of data providing 40 channel-months of observations spanning the period September 1962-September 1963. The model covered the L region 1.2-3 R_e and the energy range from 0.3-7 MeV. The spectral information was derived from the instruments of West and Imhof, while the data of McIlwain and Brown provided a better picture of the spatial distribution. The coordinate system used was the B, L system that all experimenters were employing in their data reduction and analysis processing. The Jensen and Cain magnetic field model with an epoch of 1960 was used throughout the period when trapped radiation data were collected for all the AE/AP models. The epoch assigned to AE-1 was July 1963, but a specific decay model for Starfish electrons was not given as part of the model. The energy spectrum was given as an integral spectrum since the spectral data were not accurate enough to present a differential spectrum of any meaning. To the accuracy of the data, as determined by the intercomparison of data sets, the energy spectrum was independent on the magnetic field strength B.

The model was presented as the omnidirectional integral flux, J, being given as

$$J(>E,B,L) = F(B,L)N(>E, L)$$

where F is the distribution function at E > 0.5 MeV, the energy where N is normalized to 1. N is the spectral function. The low altitude cutoff of the model was made by having the flux level of 10^3 electrons/cm^2-s for E > 0.5 MeV follow the h_{min} = 0 km line.

No attempt was made to represent the longitudinal variations at low altitude, since there was inadequate coverage. One of the main tools that had to be developed to proceed with the devel-

opment of AE-1 was the conversion program to transform directional flux to omnidirectional flux and vice versa. Since no measurement provided the distribution over a whole field line, an extrapolation method that provided the fraction of the answer resulting from real data was developed. Five of the data channels provided directional (PERP) information; the rest were omnidirectional. The manner of determining the most suitable threshold energy for a threshold detector based on its efficiency versus energy calibration was developed at this time. This method was used throughout TREMP. It was not possible to get a good measure of the spectrum based on the threshold detector channels used for AE-1. The spectrum selected was a tabular one with an exponential tail to reflect a modified fission spectrum. The comparison of the data with the model was worked out for AE-1 and since then was employed in TREMP. Basically, one uses N, the spectral function above, to divide into the experimental flux and compare this with the distribution function F. Differential spectral flux measurements were converted to integral flux using the model spectrum. This model was first presented to the community at a conference in Gatlinburg, Tennessee, in 1964 (Vette, 1965a). The full description was given in the first volume of a NASA Special Publication (NASA SP-3024) series (Vette, 1966a). A set of geomagnetic geometry tables useful for working with the data was published as a NASA Contractor Report (Vette and Porjes, 1966). The first conveyance of a model was accomplished through a letter to distribution, and card decks containing the model numerics were provided on request. AE-1 was available to users in the fall of 1964. The lag time for a NASA SP was about one year.

The AP-1, AP-2, and AP-3 Models

At the outset of constructing the first proton model, it was hoped that the energies above 15 MeV could all be encompassed in a single model. Since CRAND was believed to be the most likely source, this seemed to be a good initial approach. As the data were studied, it became apparent that the spectral behavior was B as well as L dependent. Moreover, each band had a different dependence. In order to keep the numerical size of the model consistent with the size of the 1960s computer memory, etc., this portion of the proton energy spectrum was broken into three energy ranges: 15-30 MeV, 30-50 MeV, and above 50 MeV in order to do the modeling. In this manner it was possible to represent the integral spectrum as an exponential where the exponential parameter was a function of B and L. This resulted in models of the form

$$J(>E, B, L) = F(B, L) \exp((E_1-E)/E_o(B,L))$$

In this manner the two tabular functions F and E_o were functions of two variables and could be kept to a reasonable size for computers. The value of E_1 corresponded to the integral energy associated with F, the distribution function. The proton models were numbered consecutively as they were constructed. AP1 covered the 30-50 MeV range, AP-2 the 15-30 MeV range, and AP-3 the above-50 MeV range.

Most of the data fell into the 30-50 MeV interval, so it was natural to get this in order first. The calibration of proton detectors was not as critical as for electron detectors since threshold energies or energy windows could be checked by reasonably straightforward calculations. Five satellites with a total of five instrument sets provided six channels of data amounting to 33 channel-months within the July 1958-September 1963 time period. The satellites were Explorer 4, Injun 1, Explorer 15, Relay 1, and Injun 3. All of the measurements were omnidirectional and four were threshold or integral energy measurements. The other two were 40-110 MeV bands or RAN, as used in Table 1. The distribution energy was chosen as 34 MeV since McIlwain's Relay 1 detector provided the largest spatial coverage. The L range for the model was 1.17-3.15, with the outer boundary being determined where the flux dropped to 1 proton/cm^2-s. The known time dependences of protons at that time were a solar cycle effect and a nonadiabatic redistribution resulting from large magnetic disturbances. The data showed some indication of the solar cycle effect with the low altitude data of 1958-1961 lower than the later data. The solar cycle variation was anticipated by assigning an epoch to the

models. This was September 23, 1963, to avoid the large redistribution of greater than 34 MeV protons on Relay 1 occurring on that date. These fluxes were known to be returning slowly to normal. No effect was seen below L = 1.8, but at L = 2.4 there was a decrease of about a factor of 8, except for a small region near the equator. There the effect was much smaller. It was not known then how long it would take for such effects to recover. The spatial variation of the spectrum was such that there was a significant hardening for L = 1.2-1.9 as the mirror point went to low altitude. At higher Ls there was no change with B but the spectrum softened with increasing L.

For AP-2 there was only one data set with one available channel, 18.2-35 MeV, that of McIlwain on Relay 1 covering the period May-September 1963. The distribution function was chosen at 15 MeV and the AP-1 distribution function was used with these data to obtain the spectral function. This had the same spatial character as the AP-1 spectral function. The model covered the L range 1.17-3.5. The epoch was the same as AP-1.

The data situation for AP-3 was not as bad as that for AP-2. There were four satellites—1962 AY1, 1962 BE1, Telstar 1, and Midas 5—that provided four channels of data covering 4.5 channel-months within the April 1962-February 1963 time period. In addition, some spectral information was obtained from the literature, as opposed to having the data, to help determine the exponential spectral function. For AP-3 below L = 2, the spectrum hardened as one approached the equator. The distribution function energy was 50 MeV, the epoch was September 22, 1963, and the L range covered was 1.17-2.9. Fluxes for energies up to 300 MeV were computed. Although these models were developed after AE-1, they were published along with AE-1 and AP-4.

The AP-4 Model

Although data were available for modeling down to 1 MeV, the spectral function differences dictated that a 4-15 MeV range was the next step. This was accomplished using data from 1962 AY1, 1962 BE1, Explorer 15, and Relay 1. These provided five separate channels of data covering 13 channel-months within the September 1962-September 1963 time period. All these measured protons near 5 MeV. Some of the lower energy data on these satellites mentioned in Table 1 (see page 34) were used to help determine the spectral function. This spectral function showed hardening at high B until L = 3 was reached. The distribution function energy was 4 MeV and the epoch was the same as all the previous AP models. The L range covered was 1.17-4.6. Unfortunately, the four proton models were not joined at the energy boundaries to make a smooth change from one model to the other. This was not accomplished until AP-8 was constructed as a single model encompassing all energies. Kluge and Lenhart at ESA did do some smoothing with the card decks in the late 1960s.

The AE-2 Model

Since protons below 4 MeV did not present a radiation hazard (cover glass for solar arrays stopped them), a proton model below 4 MeV was deferred. The next model, AE-2, was concerned with both inner and outer zone electrons. A report on the Starfish residue one year after the AE-1 epoch was desired, and it was time to begin the development of the outer zone electrons. A similar diversity of new data to that for AE-1 was available from the five satellites Explorer 14, 1963-38C, ERS 13, P11-AS, and OGO 1. These, along with previous data from STARAD, Injun 3, and 1963-42A collected for AE-1, were used. All told, this consisted of nine instruments providing 62 data channels which supplied 221 channel-months of data within the October 1962-June 1965 time period. The earliest data used in AE-1 were not used again in the inner zone because of the decay corrections. Four of these instruments provided good spectral data, and the others were threshold devices that provided good mapping of the B,L space. The first order spectrum obtained from the spectrometers was adjusted slightly in some

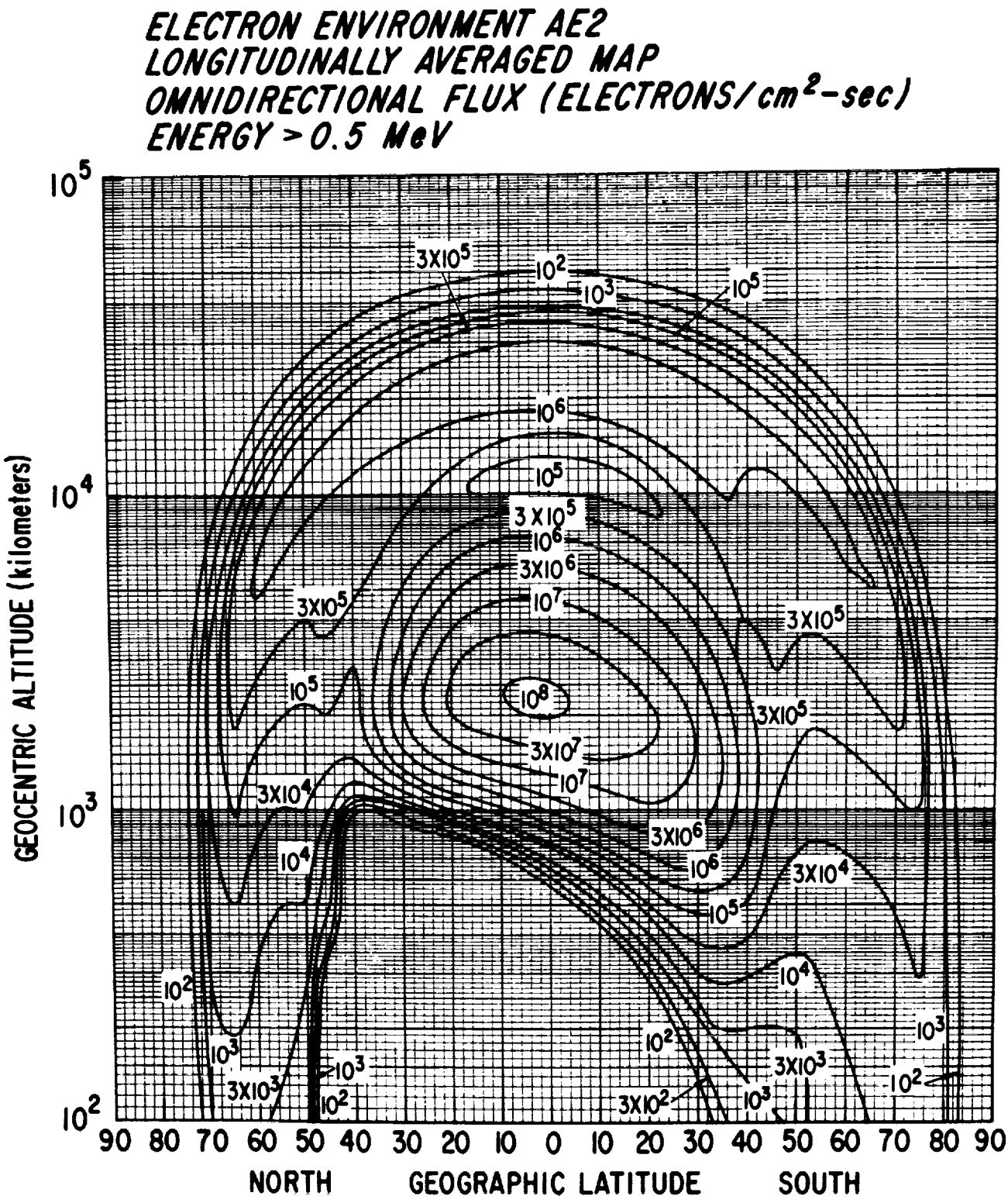

Figure 1. Longitudinally Averaged AE-2 Model.

regions to bring all the data into better agreement. The STARAD spectrometer was used only in the outer zone, since its inner zone spectrum was no longer valid in the new epoch.

The approach taken for inner zone AE-2 was similar to that for AE-1. The spectral function was tabular and no B dependence was ascertained. The 0.5 MeV distribution function energy was chosen to be consistent with AE-1. Decay values from the 1963-38C data were used to bring the other data to the August 1964 epoch. It was still not possible to introduce a decay model for this region along with the distribution and spectral model because the resulting product would contain large errors. The approach was to issue a new model in another year or two. This, of course, was not to be; the next inner zone issuance would not occur for a number of years.

The outer zone was another matter; the enormous time variations of several orders of magnitude explained in chapter 5, pages 15-20, were not easy to cope with. The approach was a very crude one, but the pragmatism of needing an outer zone electron model at this time necessitated it. Since nearly all the data plotted by investigators versus time was the logarithm of the flux (Z), it was efficient to obtain the time average of this quantity over the periods of coverage. The determination of the threshold energy of such detectors had to be done carefully for this region of space. Those instruments for which calibration data were not available were not very useful because the threshold value was spectrum dependent and this varied considerably over the L = 2-6.3 region covered.

In general, the instruments that provided good spectral data had limited spatial coverage. Threshold instruments provided the spatial coverage. It was clear that the more difficult it was to process the data from an instrument, the more selective were the intervals chosen for such processing. Solar-terrestrial physics, of which magnetospheric physics is a part, processes data on an event-oriented basis. Modeling efforts need the astronomy approach—processing all the data. Before tackling the outer zone it was realized that the B, L coordinate system lost its physical basis because of external current systems in the tail and on the magnetopause surface as well as the ring current itself in the outer zone. However, from a user standpoint a more complicated coordinate system was not desirable. In addition, there were only crude models of external fields at this time. For these reasons the same B, L coordinate system was used for AE-1 and AE-2. Local time effects were ignored because of the large time variations. The energy range for the AE-2 model was from 0.04-7 MeV and the spatial coverage was L = 1.1-6.3. This model was made available to users in the fall of 1965. The geostationary region was avoided since a more refined treatment was planned for this. In the NASA SP (Vette et al., 1966) a set of orbital integration tables for circular orbits ranging from 150-18,000 n. mi. at 0°, 30°, 60°, and 90° inclinations was included for the first time. Also included was a 1968 (SOLMAX) projected orbital integration table based on a very crude estimate of an outer zone solar cycle effect and the decay of Starfish.

AE-2 was prepared later in a special form that was never done for the other TREMP models. This was the longitudinally averaged map. Since this map shows the effect of the SAA on flux contours in a unique quantitative fashion, the results, which were never published, are shown in Figure 1 (see page 24). Notice that the altitude scale is logarithmic so that the outer zone peak appears, but the anomaly effect is quite apparent. The horns in the outer zone are also distinctly seen.

The AE-3 Model

In keeping in touch with the user community, there was a clamor to know what the environment was in the geostationary orbit region. As this work started in the beginning of 1966, there had not been a geostationary satellite that carried a set of radiation particle instruments. The first such satellite was ATS 1, which was launched in December 1966 just after AE-3 was completed. Although it was realized that the geostationary position covered a small range of L values around 6.6 (because of the parking longitude), it was decided to restrict the data base to this single L value. On the other hand, the local time variation along with the B variation would be studied. In effect, AE-3 used a three-dimensional spatial coordinate

system, the B/B_o, L, Φ system, where Φ is the geographic local time. It is convenient to use $b = B/B_o$ to simplify the notation. It was found that b was a more convenient parameter to gauge where one was in relation to the geomagnetic equator. B and L were still determined using the Jensen and Cain coefficients. The experimenters were still using these coefficients to organize their data even in the outer zone, so it was easy to convert to the new system.

The approach was to study the time behavior from six sets of instruments on six satellites that crossed the L = 6.6 shell in the time interval from August 1959 to November 1965. The satellites were Explorer 6, Explorer 12, Explorer 14, Interplanetary Monitoring Platform (IMP) 1, OGO 1, and ERS 17. They provided 16 channels with 112 channel-months of data. There were large time gaps in this long interval since most satellites did not have long operating lifetimes in those days. The low altitude portion of this L shell was not included in this investigation. For each crossing of the L = 6.6 shell, flux values were obtained along with the nominal internal magnetic field value, and the local time was computed. An iterative procedure was used to obtain the b and Φ dependence of each data set. Then the time behavior was studied by using these dependences to move the data points to the magnetic equator at local noon. Next, the time average of these projected data was determined assuming that each observation was an independent one; this neglects the knowledge of rises and decays seen in the outer zone. The time averaged omnidirectional flux model was expressed as

$$J(>E,b,\Phi) = C^{*}A(\Phi)\,b^{-m}E^{N(\Phi)}\exp(-E/E_o)$$

The energy range covered was 0.01 to 5 MeV. Values of A and N were given for each hour of local time. A dependence of the b distribution with energies below 0.2 MeV seen in the data was not incorporated into the model. Since the data covered SOLMAX and SOLMIN periods, it was estimated that the constant C had the value 9×10^7 at SOLMIN and half that value at SOLMAX. Since the error in C was about a factor of 2, it was concluded there was not a significant solar cycle effect at this L value. The functions A and N were tabular; N = 0.625 and E_o = 0.215 MeV.

From looking at many outer zone time plots of the Z, it was clear that Z bore some symmetry about its mean value. Thus, a lognormal distribution was found to be a very good fit for the cumulative distribution of points for each data set. The mean and standard deviation (σ) of each data set was determined. The value of σ increased smoothly with energy. This use of the lognormal distribution is probably the most important result coming out of this work for future modeling purposes. AE-3 was also notable in first showing the absence of a solar cycle flux effect, which has been borne out by the data of the succeeding 13 years. Finally, in comparing the results with AE-8 the AE-3/AE-8 ratio at 0.04, 0.50, and 1.0 MeV is 1.1, 1.7, and 1.0. At higher energies AE-3 drops off much faster. This model was published by Vette and Lucero (1967), although the NASA SP that was initially distributed indicated that Vette, Lucero, and Wright were the authors.

It can be seen from the construction of AE-3 that the closer the modeler tries to approach reality, the more data processing is required and the effort to produce the model increases. AE-3 required about two person-years to produce, which is about twice that of the previous models.

The AP-5 Model

In an effort launched prior to the completion of AE-3, King (1967) assembled the proton data from seven instruments flown on Injun 1, Explorer 12, Explorer 14, Relay 1, P11-AS, and Explorer 26. These provided 63 channel-months of data through 28 channels within the period July 1961-April 1965. All of the instruments provided directional fluxes; this was the first time that a model data base had such homogeneity. The AP-5 model covered the energy range 0.1-4 MeV and the L region from 1.2-6.6. Lower energy protons were not considered useful in radiation effects, so it was decided at the outset of TREMP not to include the plasma regime. King found that an exponential spectrum and a power law spectrum were equally adequate to

represent the data but used the exponential form to conform with the earlier AP models. Time variations and the agreement of the different data did not allow one to assume an accuracy better than a factor of 2, which seems to be the lower limit for trapped radiation models of this variety. Larger time variations for L > 4.5 were evident in a few cases but adequate coverage to use the AE-3 approach was not possible. It is likely in retrospect that the proton flux in the L = 3-6.6 region may be too high since the detectors in that era could not exclude the higher atomic-charged particles, which are significant during times when the ring current is enhanced. On many occasions alpha particles may reach flux levels larger than proton fluxes.

The end of the Aerospace era came with the completion of AP-5. Eight models were completed over a period of about three years using approximately nine person-years of effort. Thus, the average effort per model was about one person-year.

The AP-6 Model

The first work initiated by TREMP at NSSDC in 1967 involved AE-4. However, two proton models initiated later were finished first. Some new data were available to TREMP in the 4-30 MeV proton range by 1968. These were supplied from Telstar 2, ERS 13, and P11-AS. The Relay 1 data from McIlwain/Fillius in the 18.2-35 MeV range had been provided in two channels, 18.2-25 and 25-35. The other data from 1962 AY1, 1962 BE1, Explorer 15, and Relay 1 used in AP-2 and AP-4 were also used. Thus, seven satellites with eight instruments providing 12 channels and 55 channel-months covering the period September 1962-December 1965 were used to generate AP-6. Lavine and Vette (1969) were able to use a power law spectral function of the form

$$N(>E;\ B,L) = (E/E1)^{-P(B,L)}$$

to bring this energy range into one model covering the L range 1.2-4.0. The distribution function energy was chosen as 4 MeV. Although newer data had shown more examples of temporal changes with some being adiabatic and others nonadiabatic, there was no way to model such changes. Adiabatic changes restored fluxes in periods of days and nonadiabatic effects produced changes up to a factor of 10 in restricted regions. The new model favored 1964 data after the September 23, 1963, redistribution. Thus, an epoch of December 1964 is appropriate for AP-6; no epoch was quoted in the publication, however. Usually, the time variations were no more than the variation of disagreement in data sets; however, there is no question such changes are real. At that time the solar cycle effect, as seen in the literature, was masked by a proton redistribution caused by Starfish. The TREMP approach was to produce a static model and to summarize the literature on proton time variations.

The AP-7 Model

This model has a similar story to that of AP-6. New data dictated an update to AP-3. An attempt was made to combine AP-1 and AP-3 into a single model above 30 MeV. However, as shown previously, the spectral functions for these two energy regimes have different spatial characteristics. Eight new satellites provided new data so that the full complement came from Midas 3, Explorer 12, Midas 4, Midas 5, Telstar 1, 1962 AY1, 1962 BE1, 1963-42A, P11-AS, Gemini 4, Gemini 7, and OV3-4. This totaled 12 instruments with 22 channels that provided 26 channel-months of data within the July 1961-July 1966 time period. An exponential spectral function was used for AP-7, and the energy range 50-500 MeV was covered. The spatial extent of this model was L = 1.15-3.0 and the epoch was January 1969. This epoch was chosen because it was estimated that by that time that the equatorial bump around L = 2.2 seen by Explorer 15 and Explorer 26 for 40-110 MeV would have disappeared and that the May 1967 redistribution would have returned to pre-storm conditions. The OV3-4 data agreed with the pre-September 23, 1963, data from Relay 1, so it was concluded that perturbation had disappeared in less than

three years. Emulsion measurements were starting to show a drop in the low altitude fluxes as the rise to SOLMAX started in late 1966. It was still too early to attempt a solar effect for the protons.

The documentation for AP-7 (Lavine and Vette, 1970) brought to a close the NASA SP 3024 series as far as the models were concerned. A final volume contained a set of four papers from a symposium convened by Vette that addressed the long-term time variations of the trapped radiation environment. The future modeling effort carried out at NSSDC appeared as NSSDC publications. The faster turn-around time for these documents and the longer development time for the models led to this decision. In addition, separate support for TREMP ceased about this time, and the work was considered thereafter as part of the regular NSSDC activity.

The AE-4 Model

This was issued in August 1972 by Singley and Vette (1972a) and covered the L region 3-11 R_e and the energy range from 0.04-4.85 MeV. Eleven satellites provided 13 PI instruments containing 31 channels that delivered 321 channel-months of data during the July 1959-February 1968 time interval. The form of the model was similar to AE-3 with a few refinements. There were two epochs, 1964 and 1967, associated with SOLMIN and SOLMAX conditions, respectively. This effect was only operative in the L = 3-5 to 5.5 region, but it was clearly discernible using the OGO 1/3 intercalibrated instruments of Winckler. A low altitude cutoff was used that was analytical instead of being determined by data, because of the incomplete coverage of this region provided by the then available data. This corresponded to the h_{max} = 200 km and at that point the flux was about 1 electron/cm^2-s. The form of the model gave the time averaged omnidirectional flux above energy E as

$$J[>E,b,L,\Phi,T] = N_T[>E,L]\Phi_T[>E,L,\Phi]G[b,L]$$

where T refers to the epoch. The local time function was of the form

$$\Phi_T\ (E,L,\Phi) = K_T(E,L)\,10^{C_T(E,L)\cos((\Phi-11)\pi/12)}$$

down to L = 5 at which point no local time effects could be ascertained. The spectral function $N_T[>E,L]$ was tabular and the field line function G[b,L] was of the form

$$G[b,L] = \begin{cases} b^{-m(L)}\left(\dfrac{b_C(L)-b}{b_C(L)-1}\right)^{m+1/2} & ; \ b < b_C \\ 0 & ; \ b \geq b_C \end{cases}$$

where b_c is the cutoff value. G is normalized to 1 at b = 1, the geomagnetic equator; the first factor in G is the field line function used in AE-3. The second factor gives a cutoff function analytically useful to express the directional flux. The local time function is normalized so the average over local time is 1; this defines $K_T(E,L)$. Thus, the flux at the equator averaged over local time is given by $N_T[>E,L]$. The parameters, $C_T(E,L)$ and $m(L)$, for AE-4 were obtained using a nonlinear least squares program and the logarithm of the flux. The results were equivalent to those obtained by the iterative technique employed in AE-3, which was more descriptive by providing intermediate outputs. Using these results, the value of $N_T[>E,L]$ was obtained by

$$N_T[>E,L] = J_{expr}[>E,b,L,\Phi,T]/\Phi_T[>E,L,\Phi]G[b,L]$$

where J_{expr} was the experimental data. The quantity $N_T[> E, L]G[b, L]$ constituted the numerical model distributed in a new format consisting of a BLOCK DATA Statement (BDS). This BDS will be discussed in the chapter dealing with AP-8 and is the format used by all the models starting with AE-4. Program MODEL was developed to decode the BDS and compute the omnidirectional integral or differential flux for a given E, B, and L. The epoch 1967 model (AE-4MAX) was combined with AE-5 to form a complete inner and outer zone electron model. The statistical approach demonstrated during the AE-3 analysis was developed into an auxiliary model. The σs as a function of energy and L were provided in the documentation but a computerized version was not distributed. No b or Φ dependence could be ascertained in σ.

The comparison of the model with the data was published later (Singley and Vette, 1972b). The treatment for time variations for AE-4 was the most sophisticated developed by TREMP for outer zone electrons. AE-8 would have a few refinements in other areas but not in this. The effort to develop AE-4 involved about nine person-years over a four-year period.

The AE-5 Model

This inner zone model utilizing data from five instruments flown on 1963-38C, OGO 1, Explorer 26, OGO 3, and OV3-3 covering the time interval December 1964-December 1967 was developed by Teague and Vette (1972) in parallel with AE-4. There were 22 channels and 375 channel-months of data available for analysis. The region covered was L = 1.2-2.8, and the energy range was 0.04-4.0 MeV. Along with AE-4, the complexity of AE-5 was considerably greater than that of previous models. This model, similar to AP-5 in that all the data were directional measurements, was developed in the unidirectional form and then converted to omnidirectional flux. Three time effects were modeled: magnetic substorms, SFD, and solar cycle flux effect. For electrons below 0.7 MeV the main temporal effect was due to solar cycle changes. For energies above 0.7 MeV substorm effects had to be taken into account at the higher L values. The Starfish residue was a factor for L values 1.3-1.5 and energies 0.5-3 MeV. The model provided quiet time fluxes, meaning that there were no substorm injections present. This was the first electron model that incorporated a B dependence in the spectral function. To fix the solar cycle effect and the Starfish residue, an epoch date of October 1967 was chosen. This corresponded closely to the 1967 epoch date for AE-4MAX. Another feature of AE-5 was the determination of the atmospheric cutoff of the flux. This ties in nicely with the outer zone cutoff determined ten years later in completing AE-8. This model brought many different pieces together. The NSSDC group had developed a number of computer tools so that the models were available in several different forms. For example, AE-5 was also available in computer form as unidirectional differential energy flux. Since the making of the model required more detailed analysis, the intermediate forms could be provided. A document by Teague et al. (1972) provided the details of such programs. Unfortunately, other NSSDC work prevented the group from continuing the development of these added services to a more user-friendly level.

The Starfish Decay Model

This work involved determining the residue of Starfish for the epoch September 1964, the exponential decay time, τ, and the time when the residue flux would be equal to the quiet time natural flux. It was considered that the flux was composed of the Starfish flux, the quiet time flux, and the substorm injected flux. Data from Explorer 4, Explorer 12, 1963-38C, OGO 1, Explorer 26, Pegasus 1, Pegasus 2, OV1-2, OGO 3, OV3-3, and OGO 5 were used. The time period of the data covered July 1958-January 1969; the pre-Starfish data were used to provide upper limits to the natural inner zone electron fluxes. The 11 instruments provided 37 channels of information and contributed 629 channel-months of data. The L range was from 1.3-2.2. This work utilized some of the work accomplished in making AE-5 and was published by Teague and Stassinopoulos (1972). The geometric factors for the OV3-3 spectrometer were increased by a

factor of four by Vampola from those used in the AE-5 model. This was taken into account in the Starfish decay work.

The AE-5 1975 Projected and the AE-6 Models

Now that an inner zone Starfish residue model with decay times existed, the natural flux had been estimated, and a solar cycle flux effect had been ascertained, it was possible to project the inner zone into the future. The AE-4 model, with epochs of 1964 and 1967, provided SOLMIN and SOLMAX versions. Thus, it was appropriate to produce these versions for inner zone electrons and to merge with AE-4 to form a complete electron model. Corrections to AE-5 were needed to account for the OV3-3 changes. The AE-5P model was obtained from the corrected AE-5 by removing the Starfish component from AE-5 using the Starfish decay model, adjusting the solar cycle dependent fluxes to a solar minimum condition, and merging with AE-4MIN using the L = 2.5-2.9 region to blend them together. By this time all Starfish electrons should have disappeared from the radiation belts. The discussion of this model (Teague and Vette, 1974) includes the comparison with some new data sets available for modeling but not used in the construction of AE-5P. The model covered the L range 1.2-11 and the energy range 0.04-5.0 MeV.

By 1976 it was time to provide a model to cover the coming 1980 SOLMAX. This was accomplished by correcting AE-5 for the OV3-3 calibration change and then removing the Starfish residue present in October 1967. This inner zone portion was then merged with AE-4MAX. The publication (Teague et al., 1976) dealt mainly with the inner zone portion since there were no changes in AE-4.

The AP-8 Model

This model was issued in December 1976 (Sawyer and Vette, 1976) after four years of work involving a total of about nine person-years. It resulted from the analysis of 29 instrument sets, providing 101 channels, flown on 24 satellites that partially covered the time period from July 1958-June 1970. There were 264 channel-months of data available for the production of the model. Most of the data were used previously in the production of the AP-1-7 models. The satellites involved were Explorer 4, Injun 1, Explorer 12, 1962 AY1, 1962 BE1, Telstar 1, Explorer 14, Explorer 15, Injun 3, Relay 1, Telstar 2, 1963-38C, 1963-42A, ERS 13, P11-AS, Explorer 26, Gemini 4, ERS 17, Gemini 7, OV3-4, OV3-3, Injun 5, OV2-5, and Azur. Particularly useful new data came from OV3-3 and Azur.

AP-8 is a static model except for the solar cycle dependence afforded by the incorporation of Azur data and the work of a number of investigators who studied the processes involved in understanding the effect. The effect is too small to warrant trying to describe changes on a year-by-year basis until long-term observations by a single satellite or intercalibrated instruments on time-overlapping sensors are available. Other time variations that have been observed are pointed out in the document, but it was not possible to incorporate these into the model. Flux levels near local noon have been favored for L values above 4 to provide a pessimistic model in those regions where local time variations are present. The energy range covered is 0.1-400 MeV (so it is the first complete proton model constructed), and the L range is 1.15-6.6. The model will produce flux values at higher L values since interpolations between 6.6 and the minimum flux level at L = 10 are done. The spectral function in the model is tabular. In working with the data a differential spectral function consisting of the sum of two exponentials with six coefficients was useful but not accurate enough for the final model. More effort has been expended in modeling electron time variations because of the quantitative effect on those models and the longer data bases available for this particle.

The incorporation of the model into one large numerical storage has been convenient from a user standpoint now that computer memories are large enough. The storage format of the BDS uses the first eight locations to give the model name (two cells), epoch year, scaling factor for energy, scaling factor for L value, scaling factor for b increment corresponding to a fixed decrement in Z, scaling factor for Z1 (the equatorial Z value), and length of data array minus 1. The scaling factors for AP-8 are 100, 2048, 2048, and 1024, respectively. This permits the stored values to be integers. The storage requirements for AP-8MAX and MIN are 16,304 and 16,591, respectively. The L grid has guard values at 0, 1.14, 10, and 16; this means that the equatorial Z = 0. Then there are L values every 0.1, starting at L = 1.2 continuing through 6.6. In addition, L = 1.15 and 1.17 are included. The energy grid is 0.1, 0.2, 0.4, 0.6, 0.8, 1, 2, 4, 6, 8, 10, 15, 20, 30, 50, 60, 80, 100, 200, and 400 MeV. What is not apparent from the BDS is the fixed decrement in Z; it is 0.25 for AP-8. Sawyer also prepared a smaller version of AP-8 called AP-8MAC and AP-8MIC, each of which requires 6,697 and 6,518 storage locations, respectively. These are used when the full storage requirements are difficult to meet. In the present era meeting these requirements is usually not difficult. AE-8MAX and MIN require 13,556 and 13,176 locations, respectively; a short version does not exist.

The production of differential forms (in angle and energy) can be provided, and a matrix for unidirectional flux was made during the production of AP-8. The differential forms do not have the same validity as the basic model and contain some peculiar bumps, since the models were not built in a way that insures smooth derivatives.

The Non-Model AEI-7

In the ensuing period after AE-6 was developed, Vampola analyzed his data obtained on OV1-19 with two beta-ray spectrometers. This produced a flat differential energy spectrum for outer zone electrons above 1.5-2.0 MeV extending to the limit of the instrument. He developed two levels based on substorm injections and quiet time conditions, which differed by a factor of ~ 10. AEI-7 was an attempt by Teague to accommodate Vampola's results within AE-6 as an interim version of a new model. The HI version added Vampola's storm levels, and the LO version was a quick cut using ATS 6 and staying with more conventional data at other L values. It was becoming clear that the high energy portion of AE-4 above 2 MeV was too low, based on the ATS 6 results. The OV1-19 data became available for modeling in 1978, and it was shown by Vette's analysis later that the fluxes above 2 MeV were due entirely to background. At that point (around 1980) AEI-7 HI was withdrawn from distribution, and it was decided to call the new electron model AE-8. There was never any formal publication of AEI-7 since it was not the policy of TREMP to give false credibility to modeling work that had not been properly verified.

The Inner Zone Electron Study

This study was done to compare a number of new data sets with the data used in AE-5, except for Explorer 26, and then make comparisons with AE-5 and the inner zone portion of AE-6. The new data came from OSO 4, OGO 5, OV1-13, and OV1-19. Thus, there were data from eight instrument sets involving 44 data channels that supplied 465 channel-months of data. Except for the OGO 1 and OGO 3 data, the same normalized, energy-dependent equatorial pitch angle distribution could be derived from each data set. The OGO data had a flatter distribution. All the data were then projected to the equator so that the various time variations could be seen for the total coverage provided by these data over parts of the period September 1963-February 1970. It was concluded that with a few exceptions the data were in good agreement. It was also evident that Starfish electrons were still present in the L = 1.3-1.5 range for energies in excess of 0.5 MeV. Comparison with AE-6 was very good so that the SOLMAX fluxes of 1980 should be well represented by AE-6. This work was published by Teague et al. (1979). The study of time variations of electrons both in the inner and outer zones by TREMP is best summarized in an article by Chan et al. (1979), and the latest work on inner zone processes was applied in the IZS.

The AE-8 Model

This model was issued in its computer form in December 1983 but was not documented until recently (Vette, 1991). The model consists of three parts: (1) an inner zone that covers the L range 1.2-2.4, (2) an outer zone that covers the L range 3-11, and (3) a transition region for $2.4 < L < 3.0$. For each part there are two versions, SOLMAX and SOLMIN, to handle the solar cycle effects. AE-5P and AE-6 are used in the inner zone unchanged from the descriptions given earlier.

In the outer zone AE-4 was used as a starting point, but some significant changes were made using some new data. These data came from Vampola's spectrometer on OV3-3, Vampola's spectrometers on OV1-19, Hovestadt's threshold detector on Azur, McIlwain's experiment on Applications Technology Satellite (ATS) 6, and Paulikas' experiment on ATS 6. With the last two, a good spectrum up to 4 MeV in the geostationary region was obtained. The Azur data were useful in establishing the low altitude cutoff of the fluxes that tied in well with inner zone cutoffs. Also, the local time variation was traced down to $L = 3$, extending this variation down from $L = 5$ for AE-4. The field line function was the same form as used in AE-4; the m parameter was the same but the b_c parameter was different. An analytical description of this cutoff is given in the documentation. Using the Azur data, a method was developed to make background corrections for the OV1-19 data above 1.5 MeV. With this, the L variation of the 2-4.5 MeV electrons could be established. AE-4 fluxes below 2 MeV were in agreement with the new data. The ATS 6 local time variation provided the evidence that there was no change of this with the solar cycle. Consequently, the local time variation is different in AE-8 compared to AE-4. The statistical model of AE-4 was carried over to AE-8, since the body of data that was used to develop that was significantly larger than for the new data. The statistical analysis of the new data showed no disagreement with AE-4, but the errors were larger. The solar cycle flux effect could not be addressed independently with the new data, but within errors they were in agreement.

The transition region was completely reconstructed and contains different values on the 2.5, 2.6, 2.7, 2.8, and 2.9 L shells than before, for both SOLMAX and SOLMIN. The largest changes are for energies above 1 MeV.

If one looks at Table 2 (see page 41) and compares AP-8 and AE-8, one sees that the numbers are quite comparable except that the channel-months of data used in AE-8 are five times greater. That is caused by the long-time basis for the SFD model, and the long observing time by the ATS satellites. At any rate, those numbers should provide good estimates of what it takes to keep up with the TRE in the Earth's magnetosphere. Still, the coverage in time-energy-space left much to be desired as seen by the modeler.

The parameters of the BDS for AE-8 are as follows:

Energy scaling factor	6400
L scaling factor	2100
b increment scaling factor	1024
Equatorial z scaling factor	1024
z decrement for b	0.25
Total AE-8MAX storage	13,556
Total AE-8MIN storage	13,176

Errors in the Models

The question of errors in models such as AP-8 and AE-8 is a difficult one to answer. In the first place, the question posed is usually unspecific or ambiguous. The standard type of error treatment is not really applicable. Statistical methods have been used for the outer zone electron time variations, and the parameters should be well understood. However, one could pose questions about the effect of not including the coherent information. The answer to that would be application dependent. Systematic errors are impossible to quantify. Some data sets may have problems that become apparent when they disagree with the body of other data. The resolution of those problems may never be achieved. The OV1-19 electron data caused some concern for several years before a resolution was at hand. The accuracy can only be assessed in the context of all the data available for the model. There is no true value to be had. Since a model purports to give the time-averaged omnidirectional flux at a given point in space, a perfect instrument on an orbiting satellite could not measure this parameter. If there are some data that are processed for the model but for various reasons the modeler chooses to ignore those data in arriving at the final values, do the data contribute to error? The real answer seems to be available through an approach analogous to the legal systems that use a jury of peers to judge a person.

The comparison of the data among themselves and AP-8/AE-8 can only be done by bringing everything to a common place in time, space, and energy. In general, there is no commonality in the various data sets to do this. The model, once made, does permit this. The model takes all the stress in doing this since its properties are used to bring the measurements to omnidirectional flux above energy E at the magnetic equator at the desired L value. Of course, the measurements are time averaged after the b and Φ dependences have been removed. The model spectrum is used to convert the various observations to the energy coordinate shown. Such presentations of data/model comparisons have always been provided in the model documentation to give the user some guidance as to the errors. To arrive at one number for the error is clearly phyrric, but TREMP has usually responded to the error question with the answer "about a factor of 2." Of course, the situation in the slot near L = 3.0 and for high energy electrons at geostationary draws some additional response.

Precision is another error term that is meaningless here. Since this deals with the repeatability of the measurement (the model is really the composite measurement), one form of precision could only be estimated by having another group produce a model from the same data. This is impractical and likely will never be done.

The greatest errors can be expected where steep gradients in spatial or spectral distributions exist and where the time variations are not well understood. Unfortunately, there has been a paucity of data available to construct trapped radiation models; much more would be needed to quantify the error situation.

A final type of error that will be addressed is one of use of the models. In chapter 5 (see page 14) the use of a secularly changing geomagnetic field with AP-8 was discussed. If one invoked that AP-8 should change to conserve the three adiabatic invariants, the results would be even more devastating, since particles at higher L, lower B, and lower energy would replace those occupying the initial B, L cells sampled in the orbit. On the other hand, having a user like Pfitzer who understands the situation, the model can again become useful. In short, the error in the model is not independent of the user.

Table 1. Experimental Data Used in the Trapped Radiation Model Environment Program

Experimental Group/ Principal Investigator	Satellite	Instrument	Type of Measurement	Period of Coverage	L Coverage	Nom. Energy/ Particle (MeV)	Used in Models or Studies
U. Iowa J. A. Van Allen	Explorer 4	GMTs	THD, OMNI	7/58-10/58	1.3-1.9	31p 43p	AP-1, AP-8, SFD, AE-8 AP-1, AP-8
TRW Systems A. Rosen	Explorer 6	S/PMT	THD, OMNI	8/59-9/59	2.2-8.0	0.5e	AE-3, AE-4, AE-8
U. Minnesota J. R. Winckler	Explorer 6	GMT	THD, OMNI	8-59-10/59	2.0-8.0	3.0e	AE-4, AE-8
		Ion Chamber	THD, OMNI	8/7-25/59	2.0-8.0	1.6e	AE-4, AE-8
APL C. O. Bostrom	Injun 1	302 GMT	THD, OMNI	7/61-12/61	1.3-1.7	40p	AP-1, AP-8
		SSD	RAN, DIR	7/61-12/61	1.5-2.0	1-15p	AP-5, AP-8
GSFC L. R. Davis	Explorer 12	S/PMT	THD, DIR	8/61-12/61	2.0-5.0 4.2-6.6 2.1-6.0 2.0-4.6 2.1-3.9	0.10p 0.27p 0.51p 1.00p 1.70p	AP-8 AP-5, AP-8 AP-5, AP-8 AP-5, AP-8 AP-5, AP-8
U. Iowa J. A. Van Allen	Explorer 12	GMTs	THD, OMNI	8/61-12/61	2.0-12.0 1.2-2.3 1.2-2.3	1.9e 21p 70p	AE-3, AE-4, AE-8, SFD AP-8 AP-7, AP-8
LMSC W. L. Imhof	Midas 3	S/PMT Cluster	THD, OMNI	7/61	1.5	87p 148p	AP-7 AP-7
	Midas 4	S/PMT Cluster	THD, OMNI	10/61	1.6 1.5-1.6 1.6 1.6 1.6	87p 144p 59p 95p 148p	AP-7 AP-7 AP-7 AP-7 AP-7
	Midas 5	S/PMT Cluster	THD, OMNI	4/62	1.5-2.0 1.4-1.5 1.4-1.5	59p 95p 148p	AP-3, AP-7 AP-7 AP-7
	1962 AY1	S/PMT	THD, OMNI	9/1-4/62	1.2-1.6	1.2e	AE-1

Table 1. Experimental Data Used in the Trapped Radiation Model Environment Program (continued)

Experimental Group/ Principal Investigator	Satellite	Instrument	Type of Measurement	Period of Coverage	L Coverage	Nom. Energy/ Particle (MeV)	Used in Models or Studies
Aerospace Corp. S. C. Freden	1962 AY1	SSD	RAN, OMNI	9/1-4/62	1.2-2.9 1.2-2.2	5-20p 60-120p	AP-4, AP-6, AP-8 AP-3, AP-7, AP-8
	1962 BE1	SSD	RAN, OMNI	10/9-14/62	1.2-2.5 1.3-1.9	5-20p 60-120p	AP-4, AP-6, AP-8 AP-3, AP-7, AP-8
Aerospace Corp. J. D. Mihalov	1962BE1 1962BO1	S/PMT	BREM, OMNI BREM, OMNI	10/9-14/62 11/62	1.3-1.9 1.3-1.9	eBREM eBREM	AE-1 AE-1
BTL W. L. Brown	Telstar 1	SSDs	RAN, OMNI	10/62-2/63	1.2-2.3	26-33p 50-75p	AP-8 AP-3, AP-7, AP-8
GSFC/L. R. Davis	Explorer 14	S/PMT	THD, DIR	10/62-12/62	2.0-5.0 4.2-6.6 2.1-6.0 2.0-4.6 2.1-3.9	0.10p 0.27p 0.51p 1.00p 1.70p	AP-8 AP-5, AP-8 AP-5, AP-8 AP-5, AP-8 AP-5, AP-8
U. Iowa J. A. Van Allen	Explorer 14	GMT	THD, OMNI	10/62-8/63	2.0-12.0	1.6 & 1.9e	AE-2, AE-3, AE-4, AE-8
		GMTs	THD, DIR	10/62-8/63	2.0-12.0	0.04e 0.23e	AE-2, AE-3, AE-4, AE-8 AE-2, AE-3, AE-4, AE-8
LLL H. I. West, Jr.	STARAD	Spectrometer, Beta Ray(BRS)	Differential (DIF), DIR	10/62-12/62	1.3-3.0	0.325-3.25e in 5 channels	AE-1, AE-2
UCSD C. E. McIlwain	Explorer 15	S/PMT S/PMT	THD, DIF THD, OMNI RAN, OMNI	10/62-1/63 10/62-1/63	1.3-3.0 1.3-3.0	0.5e 5.0e 40-110p	AE-1 AE-1 AP-1, AP-8
BTL/W. L. Brown	Explorer 15	SSD	RAN, OMNI	10/62-1/63	1.3-3.0	4-13p	AP-4, AP-6, AP-8
U. Iowa B. J. O'Brien	Injun 3	GMT	THD, OMNI	12/62-9/63	1.2-6.0	1.9e & BREM	AE-1, AE-2, AE-4, AE-8
		GMT	THD, PERP	12/62-9/63	2.0-6.0	0.23e	AE-2
		S/PMT	RAN, OMNI	12/62-9/63	1.15-2.0	40-110p	AP-1, AP-8
BTL/W. L. Brown	Relay 1	SSD	THD, PERP	1/63-6/63	1.2-2.2	1.0e	AE-1
		SSD	RAN, PERP	12/62-6/63	1.5-3.0 1.4-2.7	2.5-3.8p 5.0-8.6p	AP-5, AP-8 AP-6, AP-8

Table 1. Experimental Data Used in the Trapped Radiation Model Environment Program (continued)

Experimental Group/ Principal Investigator	Satellite	Instrument	Type of Measurement	Period of Coverage	L Coverage	Nom. Energy/ Particle (MeV)	Used in Models or Studies
UCSD C. E. McIlwain	Relay 1	S/PMT	THD, OMNI	5/63-2/64	1.8-2.9	34p	AP-1, AP-8
		SSD	RAN, PERP	12/62-5/63	1.5-3.5	1.1-14p	AP-5, AP-8
					1.5-3.4	1.6-7.1p	AP-5, AP-8
					1.5-3.5	2.25-4.7p	AP-5, AP-8
		SSD Telescope (TEL)	RAN, PERP	12/62-9/63	1.4-2.5	18.2-25P	AP-6, AP-8
						25-35p	AP-6, AP-8
						18.2-35p	AP-2
						35-63p	AP-8
		S/PMT	THD, PERP	5/63-9/63	1.6-2.6	5.2p	AP-4, AP-6, AP-8
					1.3-2.5	0.45e	AE-1
BTL/W. L. Brown	Telstar 2	SSD	RAN, DIR	5/63-7/63	1.2-3.0	4-13p	AP-6, AP-8
APL/C. O. Bostrom	1963-38C	SSDs	THD, PERP	9/63-1/68	1.2-6.0	1.2 & 1.34e	AE-2, AE-5, AE-8, SFD
				9/63-12/67	1.2-6.0	0.28 & 0.254e	AE-2, AE-5, AE-8, SFD, IZS
				9/63-1/68	1.2-2.2	2.4	AE-8, SFD
				10/12-27/63	1.2-6.0	1.2-2.2p	AP-8
					1.2-5.5	2.2-8.5p	AP-8
					1.2-4.0	8.5-25p	AP-8
					1.2-3.3	25-100p	AP-8
LMSC/W. L. Imhof	1963-42A	S/PMT	PHS, OMNI	10/30-11/4/63	1.17-6.0	0.3-13e in 32 channels	AE-1, AE-2
					1.15-3.0	70p	AP7, AP-8
U. Calif.-Berkeley K. A. Anderson	IMP 1	GMT	THD, Scatter OMNI	11/63-5/64	2.0-12.0	0.045e	AE-3, AE-4, AE-8
		Ion Chamber	THD, OMNI		6.6	1.2e	AE-3
Aerospace Corp. J. I. Vette	ERS 13	SSD	THD, OMNI	7/64-11/64	1.6-8.0	0.7e	AE-2, AE-4, AE-8
					1.4-2.3	12-23p	AP-6, AP-8
Aerospace Corp. S. C. Freden	P11-AS	SSD Cluster	THD, OMNI	8/64	1.2-3.0	0.9e	AE-2S
					1.6-3.5	1.6e	AE-2
			RAN, OMNI	8/64-2/65	1.2-2.5	6-20p	AP-6, AP-8
					1.2-2.5	12-35p	AP-6, AP-8
					1.2-2.5	21-40p	AP-6, AP-8
					1.2-2.3	40-80p	AP-8
					1.2-2.1	80-110p	AP-7, AP-8
			THD, OMNI		1.2-2.1	80p	AP-7, AP-8

Table 1. Experimental Data Used in the Trapped Radiation Model Environment Program (continued)

Experimental Group/ Principal Investigator	Satellite	Instrument	Type of Measurement	Period of Coverage	L Coverage	Nom. Energy/ Particle (MeV)	Used in Models or Studies
Aerospace Corp. J. D. Mihalov	P11-AS	S/PMT	PHS, DIR	8/64	1.23-6.0	0.17-4.5e in 10 channels	AE-2J
					5.2-6.0	0.17-0.21p	AP-5, AP-8
					4.5-6.6	0.21-0.29p	AP-5, AP-8
					4.1-6.6	0.29-0.42p	AP-5, AP-8
					2.2-6.6	0.42-0.55p	AP-5, AP-8
					2.2-3.6	0.55-1.20p	AP-5, AP-8
					3.1-3.7	1.20-1.70p	AP-5, AP-8
					2.0-3.7	1.50-1.90p	AP-5, AP-8
					2.3-4.0	1.90-2.40p	AP-5, AP-8
					2.2-3.1	2.40-3.40p	AP-5, AP-8
U. Minnesota J. R. Winckler	OGO 1	5-Channel S/PMT Spectrometer	DIF, DIR	9/64-6/67	1.3-7.0	0.036-0.133e	AE-2, AE-3, AE-4, AE-5, AE-8, SFD, IZS
						0.133-0.292e	AE-2, AE-3, AE-4, AE-5, AE-8, SFD, IZS
						0.292-0.690e	AE-2, AE-3, AE-4, AE-5, AE-8, SFD, IZS
						0.690-1.970e	AE-2, AE-3, AE-4, AE-5, AE-8, SFD, IZS
						1.970-∞ e	AE-2, AE-3, AE-4, AE-5, AE-8, SFD, IZS
		Ion Chamber	THD, OMNI	9/64-10/65	6.6	0.7e	AE-3
UCSD C. E. McIlwain	Explorer 26	S/PMT	THD, OMNI	1/65-12/65	2.5-6.9	4.0e	AE-4, AE-8
		S/PMT	THD, DIR	1/65-12/65	2.5-7.0	0.50 & 0.52e	AE-4, AE-5, AE-8, SFD
BTL/W. L. Brown	Explorer 26	SSD Cluster	THD, Scatter OMNI	1/65-5/67	3.5-6.5	1.0e	AE-4, AE-8
						3.5e	AE-4, AE-8
						2.5e	AE-4, AE-8
GSFC/L. R. Davis	Explorer 26	S/PMT	THD, DIR	4/5-5/65	2.0-5.8	0.098p	AP-8
					2.0-5.8	0.134p	AP-5, AP-8
					2.5-5.4	0.180p	AP-5, AP-8
					2.3-5.4	0.345p	AP-8
					2.2-5.4	0.513p	AP-5, AP-8
					2.2-4.6	0.775p	AP-5, AP-8
					2.0-4.7	1.140p	AP-5, AP-8
					2.0-4.5	1.700p	AP-5, AP-8

Table 1. Experimental Data Used in the Trapped Radiation Model Environment Program (continued)

Experimental Group/ Principal Investigator	Satellite	Instrument	Type of Measurement	Period of Coverage	L Coverage	Nom. Energy/ Particle (MeV)	Used in Models or Studies
MSFC R. Potter	Pegasus 1	S/PMTs	THD, OMNI	2/65-10/67	1.3-1.5	0.5e 1.9e	SFD, AE-8 SFD, AE-8
MSFC R. Potter	Pegasus 2	S/PMTs	THD, OMNI	5/65-10/67	1.3-1.5	0.5e 1.9e	SFD, AE-8 SFD, AE-8
LMSC/W. L. Imhof	Gemini 4	S/PMT	THD, OMNI	6/3-6/7/65	1.15-1.2	64p	AP-7, AP-8
Aerospace Corp. J. I. Vette	ERS 17	SSD	THD, OMNI	7/65-11/65	2.0-12.0 1.4-4.0	0.32 & 0.40e 8-21p	AE-3, AE-4, AE-8 AP-8
		S/PMT	THD, DIR		2.0-12.0	0.1e	AE-3, AE-4, AE-8
		GMTs	THD, OMNI		6.6	0.04e	AE-3
UCLA/T. A. Farley	OV1-2	S/PMT	THD, OMNI	10/65-12/65	1.2-1.6	0.56e	SFD, AE-8
LMSC/W. L. Imhof	Gemini 7	S/PMT	THD, OMNI	12/4-12/7/65	1.15-1.2	70p	AP-7, AP-8
U. Minnesota J. R. Winckler	OGO 3	Same as OGO 1	DIF, DIR	6/66-12/67	1.3-8.0	Same as OGO 1	AE-4, AE-5, AE-8, SFD, IZS
Air Force Weapons Lab/Staff	OV3-4	SSD Cluster	THD, OMNI	6/66-7/66	1.15-3.0 1.15-2.6 1.15-2.6 1.15-2.4 1.15-2.2	15p 30p 55.5p 105.5p 170p	AP-8 AP-8 AP-7, AP-8 AP-7, AP-8 AP-7, AP-8
Aerospace Corp. G. A. Paulikas	OV3-3	SSD Cluster	RAN, OMNI	9/66-10/66	1.17-2.5 1.17-2.5 1.17-2.5 1.17-2.0 1.17-2.5	12-22p 21-40p 40-80p 80-140p 80-400p	AP-8 AP-8 AP-8 AP-8 AP-8
Aerospace Corp. A. L. Vampola	OV3-3	BRS	DIF, PERP	7/66-9/67	1.2-6.6	0.225-0.375e 0.350-0.600e 0.575-0.850e 0.815-1.100e 1.075-1.375e 1.329-1.651e 1.615-1.925e 1.880-2.200e 2.148-2.473e	AE-5, AE-8, SFD, IZS AE-5, AE-8, SFD, IZS AE-5, AE-8, SFD, IZS AE-5, AE-8, SFD, IZS AE-5, AE-8, SFD, IZS AE-5, AE-8, SFD, IZS AE-5, AE-8, SFD, IZS AE-5, AE-8, SFD, IZS AE-5, AE-8, SFD, IZS

Table 1. Experimental Data Used in the Trapped Radiation Model Environment Program (continued)

Experimental Group/ Principal Investigator	Satellite	Instrument	Type of Measurement	Period of Coverage	L Coverage	Nom. Energy/ Particle (MeV)	Used in Models or Studies
Aerospace Corp. G. A. Paulikas	ATS 1	SSD Cluster	THD, OMNI	12/66-10/68	6.6	0.3e 0.45e 1.05e 1.9e	AE-4, AE-8 AE-4, AE-8 AE-4, AE-8 AE-4, AE-8
LLL/J. A. Waggoner	OSO 4	S/PMT	PHS, DIR	3/68	1.2-1.9	0.0805-0.121e 0.121-0.171e 0.171-0.258e 0.258-0.537e 0.537-0.900e	IZS, AE-8 IZS, AE-8 IZS, AE-8 IZS, AE-8 IZS, AE-8
LLL/H. I. West, Jr.	OGO 5	BRS	DIF, DIR	3/68-1/69	1.3-2.4	0.056-0.102e 0.122-0.194e 0.230-0.302e 0.427-0.531e 0.637-1.007e 1.270-1.790e 2.550-3.090e	SFD, IZS, AE-8 SFD, IZS, AE-8 SFD, IZS, AE-8 SFD, IZS, AE-8 SFD, IZS, AE-8 SFD, IZS, AE-8 SFD, IZS, AE-8
USAF Geophysics Lab/L. Katz	OV1-13	BRS		5/68-7/68	1.2-2.4	0.140-0.180e 0.185-0.235e 0.450-0.550e 0.620-0.720e 0.850-0.950e	IZS, AE-8 IZS, AE-8 IZS, AE-8 IZS, AE-8 IZS, AE-8
U. Iowa J. A. Van Allen	Injun 5	SSD TEL	PHS, PERP	8/68-11/68	2.0-5.0 2.0-5.0 1.5-5.0 1.5-4.0 1.5-3.0 1.5-2.0 1.5-2.0 1.5-5.0 1.5-4.0 1.5-2.0 1.5-2.0	0.3-0.6p 0.6-1.0p 1.0-1.5p 1.5-2.0p 2.0-5.0p 5.0-10.0p 10.0-15.0p 0.80-1.43p 1.43-4.20p 4.2-9.2p 3.44-74p	AP-8 AP-8 AP-8 AP-8 AP-8 AP-8 AP-8 AP-8 AP-8 AP-8 AP-8
Aerospace Corp. J. R. Stevens	OV2-5	SSD TEL	RAN, DIR	10/68	6.6	0.06-3.3p 0.1-0.3p 0.3-0.6p 0.6-1.0p 1.0-1.5p	AP-8 AP-8 AP-8 AP-8 AP-8

Table 1. Experimental Data Used in the Trapped Radiation Model Environment Program (continued)

Experimental Group/ Principal Investigator	Satellite	Instrument	Type of Measurement	Period of Coverage	L Coverage	Nom. Energy/ Particle (MeV)	Used in Models or Studies
Aerospace Corp. A. L. Vampola	OV1-19	BRS	DIF, DIR	3/69-1/70	3.0-6.6	0.039-0.068e	AE-8, IZS
						0.074-0.111e	AE-8, IZS
						0.168-0.216e	AE-8, IZS
						0.224-0.276e	AE-8, IZS
						0.285-0.339e	AE-8, IZS
						0.348-0.404e	AE-8, IZS
						0.415-0.473e	AE-8, IZS
		BRS	DIF, DIR			0.423-0.656e	AE-8
						0.698-0.946e	AE-8
						1.585-1.844e	AE-8
						1.888-2.152e	AE-8
						2,192-2.457e	AE-8
						2.498-2.766e	AE-8
						2.803-3.071e	AE-8
						3.423-3.690e	AE-8
						3.725-3.999e	AE-8
						4.033-4.310e	AE-8
						4.339-4.623e	AE-8
						4.643-4.930e	AE-8
						4.955-5.243e	AE-8
UCSD C. E. McIlwain	ATS 5	S/PMT Cluster	PHS, OMNI	8/69-4/72	6.6 12	0.5-5.0e in 12 channels Used to match ATS 6	AE-8
U. Kiel J. Moritz	Azur	SSD	RAN, DIR	11/69-6/70	1.5-6.6	0.25-1.65p	AP-8
Max Planck Inst. Garching/ D. Hovestadt	Azur	SSD TEL	RAN, PERP	11/69	1.5-4.0	1.5-2.7p	AP-8
					1.5-4.0	2.7-5.2p	AP-8
					1.5-3.0	5.2-10.4p	AP-8
					1.17-2.5	10.4-22.0p	AP-8
					1.17-2.0	22.0-49p	AP-8
						49-104p	AP-8
		SSD	THD, OMNI	11/69-3/70	3.0-6.6	1.5e	AE-8
						4.5e	AE-8
Aerospace Corp. G. A. Paulikas	ATS 6	SSD Cluster	RAN, OMNI THD, OMNI	5/74-4/78	6.6	0.14-0.60e	AE-8
						0.7e	AE-8
						1.55e	AE-8
						3.9e	AE-8

Table 2. Summary of Data Usage in Trapped Radiation Environment Models*

Model Name	Satellites	Sets of PI Instruments	Data Channels	Channel-Months of Data
AE-1	8	9	45	40
AE-2	8	9	62	221
AE-3	6	6	16	112
AE-4	11	13	31	321
AE-5	5	5	22	375
AE-5P	11	11	37	629
AE-6	11	11	37	629
AE-8	24	26	95	1303
SFD	11	11	37	629
IZS	8	8	44	465
AP-1	5	5	6	33
AP-2	1	1	2	18
AP-3	4	4	4	4
AP-4	4	5	5	13
AP-5	6	7	28	63
AP-6	7	8	12	55
AP-7	12	12	22	26
AP-8	24	29	101	264
Non-Redundant Totals	43	55	265	1630

* Data covers portions of period July 1958 - April 1978.

7. References

Chan, K. W., D. M. Sawyer, and J. I. Vette, "The Trapped Radiation Population," in *The Trapped Radiation Handbook*, eds. J. B. Cladis, G. T. Davidson, and L. L. Newkirk, Defense Nuclear Agency, DNA 2524 Change 5, January 1977a.

Chan, K. W., D. M. Sawyer, and J. I. Vette, *A Model of the Near-Earth Plasma Environment and Application to the ISEE-A and -B Orbit*, National Space Science Data Center, NSSDC/WDC-A-R&S 77-01, July 1977b.

Chan, K. W., M. J. Teague, N. J. Schofield, and J. I. Vette, "Modeling of Electron Time Variations in the Radiation Belts," in *Quantitative Modeling of Magnetospheric Processes*, ed. W. P. Olson, American Geophysical Union, Washington, D.C., 121, 1979.

Farley, T. A., "Radial Diffusion of Starfish Electrons," *J. Geophys. Res.* 74, 3591, 1969.

Kaye, S. M., "Summary and Comparison of Radiation Belt Models," in *Proceedings of the Air Force Geophysics Laboratory Workshop on the Earth's Radiation Belts: January 26-27, 1981*, eds. R. C. Sagalyn, W. N. Spjeldvik, and W. J. Burke, Air Force Geophysics Laboratory, AFGL-TR-81-0311, 271, October 1981.

King, J. H., *Models of the Trapped Radiation Environment—Vol. IV: Low Energy Protons*, NASA SP-3024, 1967.

Konradi, A., A. C. Hardy, and W. Atwell, "Radiation Environment Models and the Atmospheric Cutoff," *J. Spacecraft and Rockets* 24, 284, 1987.

Hilberg, R. H., and J. I. Vette, *Comparison of the Trapped Electron Models AE-4 and AE-5 with AE-2 and AE-3*, National Space Science Data Center, NSSDC 74-13, September 1974.

Lavine, J. P., and J. I. Vette, *Models of the Trapped Radiation Environment—Vol. V: Inner Belt Protons*, NASA SP-3024, 1969.

Lavine, J. P., and J. I. Vette, *Models of the Trapped Radiation Environment—Vol. VI: High Energy Protons*, NASA SP-3024, 1970.

Lavine, J. P., and J. I. Vette, "A Recalculation of the Magnetic Coordinates for Explorer 4," *J. Geophys. Res.* 75, 1940, 1970.

Rosen, A., and N. L. Sanders, "Loss and Replenishment of Electrons in the Inner Radiation Zone During 1965-1967," *J. Geophys. Res.* 76, 110, 1971.

Sawyer, D. M., and J. I. Vette, *AP-8 Trapped Proton Environment for Solar Maximum and Solar Minimum*, National Space Science Data Center, NSSDC/WDC-A-R&S 76-06, December 1976.

Sawyer, D. M., K. W. Chan, M. J. Teague, and N. J. Schofield, Jr., "A Review of the Near-Earth Radiation Environment," in *Thirteenth IEEE Photovoltaic Specialist's Conference—1978*, Washington, D.C., 545, 1978.

Singley, G. W., *The Reduction and Analysis of Electron Data for Outer Zone Electron Data for Outer Zone Electron Model AE-4, Vol. I Explorer 26 UCSD Experiment Data*, National Space Science Data Center, NSSDC 71-06, March 1971.

Singley, G. W., and J. I. Vette, *The AE-4 Model of the Outer Radiation Zone Electron Environment*, National Space Science Data Center, NSSDC 72-06, August 1972a.

Singley, G. W., and J. I. Vette, *A Model Environment for Outer Zone Electrons*, National Space Science Data Center, NSSDC 72-13, December 1972b.

Teague, M. J., *The Calibration Constants for the OGO 1/3 Electron Spectrometer*, National Space Science Data Center, NSSDC 70-14, October 1970.

Teague, M. J., and J. I. Vette, *Variation of the Electron Spectrum in the Inner Radiation Belt, September 1964 to Present*, National Space Science Data Center, NSSDC 71-11, April 1971.

Teague, M. J., and J. I. Vette, *The Inner Zone Electron Model AE-5*, National Space Science Data Center, NSSDC 72-10, November 1972.

Teague, M. J., J. Stein, and J. I. Vette, *The Use of the Inner Zone Electron Model AE-5 and Associated Computer Programs*, National Space Science Data Center, NSSDC 72-11, November 1972.

Teague, M. J., and E. G. Stassinopoulos, *A Model of the Starfish Flux in the Inner Radiation Zone*, Goddard Space Flight Center, X-601-72-487, December 1972.

Teague, M. J., and J. I. Vette, *A Model of the Trapped Electron Population for Solar Minimum*, National Space Science Data Center, NSSDC 74-03, April 1974.

Teague, M. J., K. W. Chan, and J. I. Vette, *AE-6: A Model Environment for Trapped Electrons for Solar Maximum*, National Space Science Data Center, NSSDC/WDC-A-R&S 76-04, May 1976.

Teague, M. J., N. J. Schofield, K. W. Chan, and J. I. Vette, *A Study of Inner Zone Electron Data and Their Comparison with Trapped Radiation Models*, National Space Science Data Center, NSSDC/WDC-A-R&S 79-06, August 1979.

Vette, J. I., "The Updating and Dissemination of the Knowledge of Trapped Radiation Model Environments," in *Second Symposium on the Protection Against Radiations in Space*, ed. A. Reetz, NASA SP-71, 47, 1965a.

Vette, J. I.,"The Space Radiation Environment," *IEEE Trans. Nuc. Sci., NS-12*, 1, October 1965b.

Vette, J. I., and H. J. Porjes, *Geomagnetic Geometry Tables*, National Aeronautics and Space Administration, NASA CR-390, March 1966.

Vette, J. I., *Models of the Trapped Radiation Environment—Vol. I: Inner Zone Protons and Electrons*, NASA SP-3024, 1966a.

Vette, J. I., "A Model Proton Environment Above 4 MeV," in *Radiation Trapped in the Earth's Magnetic Field*, ed. B. M. McCormac, D. Reidel Publishing Company, Dordrecht-Holland, 65, 1966b.

Vette, J. I., A. B. Lucero, and J. A. Wright, *Models of the Trapped Radiation Environment—Vol. II: Inner and Outer Zone Electrons*, NASA SP-3024, 1966.

Vette, J. I., "Trapped Radiation Model Environment," in *Geophys. and Space Data Bulletin, Vol. IV, A1*, Air Force Cambridge Research Laboratories, 1967.

Vette, J. I., and A. B. Lucero, *Models of the Trapped Radiation Environment—Vol. III: Electrons at Synchronous Altitude*, NASA SP-3024, 1967.

Vette, J. I., "Summary of Particle Populations in the Magnetosphere," in *Particles and Fields in the Magnetosphere*, ed. B. M. McCormac, D. Reidel Publishing Company, Dordrecht-Holland, 241, 1970a.

Vette, J. I., "Panel Report—1. Trapped Particles," in *Particles and Fields in the Magnetosphere*, ed. B. M. McCormac, D. Reidel Publishing Company, Dordrecht-Holland, 432, 1970b.

Vette, J. I., "Electrons and Protons in the Earth's Magnetosphere," *Trans. Amer. Nuc. Soc.* 13, 415, 1970.

Vette, J. I., ed., *Models of the Trapped Radiation Environment—Vol. VII: Long-Term Time Variations—Papers from a Scientific Session on Models of the Earth's Radiation Environment at the International Association of Geomagnetism and Aeronomy General Scientific Assembly in Madrid*, September 1969, NASA SP-3024, 1971a.

Vette, J. I., "Trapped Radiation Population," in *The Trapped Radiation Handbook*, eds. J. B. Cladis, G. T. Davidson, and L. L. Newkirk, DNA 2524H, Defense Nuclear Agency, 4-1, December 1971b.

Vette, J. I., "Magnetospheric Particle Populations," in *Earth's Magnetospheric Processes*, ed. B. M. McCormac, D. Reidel Publishing Company, Dordrecht-Holland, 49, 1972.

Vette, J. I., K. W. Chan, and M. J. Teague, *Problems in Modeling the Earth's Trapped Radiation Environment*, Air Force Geophysics Laboratory, AFGL-TR-78-0130, 1978.

Vette, J. I., "Overview—High Energy Particles," in *Quantitative Modeling of Magnetospheric Processes*, ed. W. P. Olson, American Geophysical Union, Washington, D.C., 118, 1979.

Vette, J. I., M. J. Teague, D. M. Sawyer, and K. W. Chan, "Modeling the Earth's Radiation Belts," in *Solar-Terrestrial Predictions, Vol. 2: Working Group Reports and Reviews*, ed. R. F. Donnelly, U.S. Department of Commerce, NOAA Environmental Research Labs, 21, December 1979.

Vette, J. I., and D. M. Sawyer, "Short Report on Radiation Belt Calculations," 1986, unpublished.

Vette, J. I. "Trapped Radiation Models," in *Development of Improved Models of the Earth's Radiation Environment, Technical Note 1: Model Evaluation*, ESA/ESTEC Contract Report/Contract No. 8011/88/NL/MAC, p. 135, June 1989.

Vette, J. I., "Trapped Radiation," in *Development of Improved Models of the Earth's Radiation Environment, Technical Note 2: Model Formalisms*, ESA/ESTEC Contract Report/Contract No. 8011/88/NL/MAC, p. 4-1, January 1990.

Vette, J. I., "Potential Model Formalisms," in *Development of Improved Models of the Earth's Radiation Environment, Technical Note 2: Model Formalisms*, ESA/ESTEC Contract Report/Contract No. 8011/88/NL/MAC, p. 6-1, January 1990.

Vette, J. I., S. McKenna-Lawlor, and J. Lemaire, *Development of Improved Models of the Earth's Radiation Environment, Technical Note 6: The Energetic Particle Radiation Environment and Definition of Flight Measurements Requirements*, ESA/ESTEC Contract Report/Contract No. 8011/88/NL/MAC, July 1990.

Vette, J. I., *The AE-8 Trapped Electron Model Environment*, National Space Science Data Center, NSSDC/WDC-A-R&S 91-24, November 1991.

Acronyms and Abbreviations

AE-5P	AE-5 Projected
AFCRL	Air Force Cambridge Research Laboratory
AFGL	Air Force Geophysics Laboratory
AGU	American Geophysical Union
APL	Applied Physics Laboratory
ATS	Applications Technology Satellite
BDS	BLOCK DATA Statement
BREM	Bremsstrahlung
BRS	Beta Ray Spectrometer
BTL	Bell Telephone Laboratories
CPA	Charged Particle Analyzer
CRAND	Cosmic-ray albedo neutron decay
CRRES	Combined Release and Radiation Effects Satellite
DIF	Differential
DIR	Directional
DMSP	Defense Meteorological Satellite Program (DOD)
ERS	Environmental Research Satellite
ESA	European Space Agency
ESTEC	European Space Technology Center
GMS	Geostationary Meteorological Satellite
GMT	Geiger-Mueller Tube
GOES	Geostationary Operational Environment Satellite
GSFC	Goddard Space Flight Center
HEPAD	High Energy Proton and Alpha Detector
IKI	Institute of Cosmic Investigation (U.S.S.R.)
IMP	Interplanetary Monitoring Platform
ISAS	Institute of Space and Aeronautical Science (Japan)
ISEE	International Sun-Earth Explorer
IUE	International Ultraviolet Explorer
IZS	Inner Zone Study
L	McIlwain parameter
LANL	Los Alamos National Laboratory
LLL	Lawrence Livermore Laboratory
LMSC	Lockheed Missile and Space Corporation
MEPED	Medium Energy Proton and Electron Detector
MEPI	Medium Energy Particle Instrument
NASA	National Aeronautics and Space Administration
NASA SP	NASA Special Publication
NASDA	National Aeronautics and Space Development Agency (Japan)
NOAA	National Oceanographic and Atmospheric Administration
NSSDC	National Space Science Data Center

OMNI	Omnidirectional
OSO	Orbiting Solar Observatory
PERP	Perpendicular
PHS	Pulse height analysis
RAN	Range
RFP	Request for proposal
S/PMT	Scintillator/photomultiplier tube
SAA	South Atlantic Anomaly
SCATHA	Spacecraft Charging at High Altitudes
SEE	Spectrometer for Energetic Electrons
SEM	Space Environment Monitor
SFD	Starfish decay
SOLMAX	Solar maximum
SOLMIN	Solar minimum
SSD	Solid State Detector
SSD TEL	Solid State Telescope
THD	Threshold detector
TIROS	Television and Infrared Observation Satellite
TRE	Trapped radiation environment
TREM	Trapped radiation environment (TRE) model
TREMP	Trapped Radiation Environment Modeling Program
U. Iowa	University of Iowa
UCSD	University of California at San Diego
USAF	United States Air Force
VLF	Very low frequency